

Award Number: W81XWH-07-1-0215

TITLE: Cellular Therapy to Obtain Rapid Endochondral Bone Formation

PRINCIPAL INVESTIGATOR: Elizabeth A. Olmsted-Davis, Ph.D.

CONTRACTING ORGANIZATION: Baylor College of Medicine
Houston, TX 77030

REPORT DATE: February 2008

TYPE OF REPORT: Annual

PREPARED FOR: U.S. Army Medical Research and Materiel Command
Fort Detrick, Maryland 21702-5012

DISTRIBUTION STATEMENT: Approved for Public Release;
Distribution Unlimited

The views, opinions and/or findings contained in this report are those of the author(s) and should not be construed as an official Department of the Army position, policy or decision unless so designated by other documentation.

REPORT DOCUMENTATION PAGE				Form Approved OMB No. 0704-0188	
Public reporting burden for this collection of information is estimated to average 1 hour per response, including the time for reviewing instructions, searching existing data sources, gathering and maintaining the data needed, and completing and reviewing this collection of information. Send comments regarding this burden estimate or any other aspect of this collection of information, including suggestions for reducing this burden to Department of Defense, Washington Headquarters Services, Directorate for Information Operations and Reports (0704-0188), 1215 Jefferson Davis Highway, Suite 1204, Arlington, VA 22202-4302. Respondents should be aware that notwithstanding any other provision of law, no person shall be subject to any penalty for failing to comply with a collection of information if it does not display a currently valid OMB control number. PLEASE DO NOT RETURN YOUR FORM TO THE ABOVE ADDRESS.					
1. REPORT DATE 01-02-2008		2. REPORT TYPE Annual		3. DATES COVERED 1 Feb 2007 – 31 Jan 2008	
4. TITLE AND SUBTITLE Cellular Therapy to Obtain Rapid Endochondral Bone Formation				5a. CONTRACT NUMBER	
				5b. GRANT NUMBER W81XWH-07-1-0215	
				5c. PROGRAM ELEMENT NUMBER	
6. AUTHOR(S) Elizabeth A. Olmsted-Davis, Ph.D., Alan R. Davis, Ph.D., Michael Heggeness M.D., Jennifer West, Ph.D., Francis Gannon M.D., John Hipp, Ph.D., Ronke Olabisi Ph.D., Mary Dickinson Ph.D., and Aya Wada, Ph.D., Email: edavis@bcm.tmc.edu				5d. PROJECT NUMBER	
				5e. TASK NUMBER	
				5f. WORK UNIT NUMBER	
7. PERFORMING ORGANIZATION NAME(S) AND ADDRESS(ES) Baylor College of Medicine Houston, TX 77030				8. PERFORMING ORGANIZATION REPORT NUMBER	
9. SPONSORING / MONITORING AGENCY NAME(S) AND ADDRESS(ES) U.S. Army Medical Research and Materiel Command Fort Detrick, Maryland 21702-5012				10. SPONSOR/MONITOR'S ACRONYM(S)	
				11. SPONSOR/MONITOR'S REPORT NUMBER(S)	
12. DISTRIBUTION / AVAILABILITY STATEMENT Approved for Public Release; Distribution Unlimited					
13. SUPPLEMENTARY NOTES					
14. ABSTRACT Not Provided					
15. SUBJECT TERMS Not Provided					
16. SECURITY CLASSIFICATION OF:			17. LIMITATION OF ABSTRACT	18. NUMBER OF PAGES	19a. NAME OF RESPONSIBLE PERSON
a. REPORT	b. ABSTRACT	c. THIS PAGE			USAMRMC
U	U	U	UU	32	19b. TELEPHONE NUMBER (include area code)

Table of Contents

Introduction.....	4
Body.....	4
Key Research Accomplishments.....	15
Reportable Outcomes.....	26
Conclusions.....	16
References.....	17
Appendices.....	18

Introduction: This project, on the use of cell-based gene therapy for the production of rapid endochondral bone formation, and fracture healing is a collaborative effort between a bio-engineering/biomaterials group at Rice University and Baylor College of Medicine. Although bone possesses the rare capacity to continually renew and repair itself, more than 500,000 bone repair surgical procedures are performed annually within the United States alone. The need to enhance or initiate bone formation in a controlled clinical manner has brought tissue engineering to the forefront of orthopedic research. Much recent effort has been directed to the identification of factors essential to normal bone formation, and the development of new osteoconductive materials that can temporarily fill areas of missing osteoid. Still lacking are effective osteoinductive components that could be seeded into the osteoconductive materials to generate normal bone which this study will explore. The central hypothesis of this application is that rapid bone formation can be successfully achieved with only minimally invasive percutaneous techniques and without a scaffold, by using cells transduced with adenovirus vectors to express an osteoinductive factor (BMP2), which have been encapsulated in hydrogel material and later photopolymerized at the desired site.

The goal of this study is to provide a safe effective system for inducing bone formation for fracture healing. This set of proposed experiments will provide significant knowledge to the field of bone tissue engineering. Proposed studies will provide essential biological information and involves the development of a novel biomaterial that can safely house the cells expressing the bone inductive factor to produce the new bone at which time the material is then selectively eliminated. Ultimately this system has significant applicability. Often bone graft must be surgically removed from the pelvis, to implant into the site of difficult fractures for proper healing. This additional surgery often results in significant pain, and long term healing. Further, this system would be applicable to orthopedic trauma situations that previously resulted in amputation. We propose in these studies to complete the development of this bone induction system and test it in a preclinical animal model. Validation of our hypothesis will provide a safe and efficacious material for the production of bone leading to reliable fracture healing, circumventing the need for bone grafts, or for direct administration of cells, viruses, or other materials that could lead to significant adverse reactions.

Body: The central hypothesis of this application is that rapid bone formation can be successfully achieved with only minimally invasive percutaneous techniques and without a scaffold, by using cells transduced with adenovirus vectors to express an osteoinductive factor (BMP2), which have been encapsulated in hydrogel material and later photopolymerized at the desired site.

Task 1: To produce high levels of BMP2 from human mesenchymal stem cells transduced Ad5F35BMP2 adenovirus in the presence of tetracycline carrying a red luciferase reporter gene.

a. *To determine if sustained expression of BMP2 is more efficient at inducing rapid bone formation than a pulse of expression using the tetracycline regulated vectors. (Months 0-12)*

These experiments have been initiated however we have run into some initial problems with the tetracycline regulated vectors being weak in the induction of the gene, and somewhat leaky thus lowering the specific tetracycline induced gene expression. So we are currently re-constructing them using the updated modified tetracycline activator protein (In Vitrogen Technologies, CA), which has been mutated and thus has much tighter binding, and has been demonstrated in the literature to result in more significant differences in transcriptional activation in the presence of tetracycline. We have since updated these vector systems. First we are testing a novel tetracycline regulatory vector which has all components on the same vector, but into two separate regions of adenovirus to avoid the problem of promoter interference. Secondly, Clontech has initiated a similar project in collaboration with us, in which the tet activator is placed in the E3 region of adenovirus, and the tetracycline regulated minimal CMV promoter in the E1 region. With this system we can have efficient attenuation of the BMP2 through tetracycline. This is a slightly altered strategy from our

previous vector in which both portions were in the E1 region. Clontech is still working on there's but has agreed to provide it to us free of charge for testing, so that we might co-develop there system. This quarter, we have started working on cloning the BMP2-dsRED system into a tamoxifen regulated system that has also had much success for temporal attenuation in *in vivo* systems.

However, once we have constructed and testing of the new BMP2 vector we will clone quickly clone this into these viruses as well. We have had significant trouble removing the 36 bp conserved region known in other proteins such as noggin to bind collagen-betaglycan. We have now employed a strategy of 9 bp deletions in a series of site directed mutagenesis steps to remove the complete region and keep BMP2 in frame. We have currently had some success with the first steps of this process, but do not have the completed clone yet. Once we obtain this we will check the BMP2 to confirm the activity, and then quickly construct the adenovirus. From there we will confirm its abilities to more readily diffuse from the hydrogel. If we observe significant improvement, then this finding can be rapidly published.

b. To determine if longer expression times of BMP2 from cells embedded in hydrogel and longer cellular viability lead to more rapid bone formation than the rapid but short burst of BMP2 release obtained from the cells directly injected. (Months 9-12)

We have currently constructed the Ad5E1BMP2 E3dsRED vector for testing initial testing. We have found that this reporter to be the most sensitive, and easiest for use in the hydrogel material. We have thus scheduled the experiments to track the injected cells and compare the temporal and spatial expression of dsRed *in vivo*, to that obtained from cells in the hydrogel material as described in Aim 1. One anticipated problem may be seeing the material through the muscle tissues. Although we can readily see the dsRED in subcutaneous delivery, intramuscular implantation may pose more challenges. Further the hydrogel may in fact shield the dsRED signal to some extent; so therefore, we may need to invoke a window system for viewing the signal *in vivo*. Please see section III for details. This will require additional animal protocol review and approval, and although these technologies are widely used in microscopy experimentation including here at BCM, this will slow down the collection of data.

c. To demonstrate the termination of BMP2 expression using an Ad5F35tet-BMP2-IRES CBRLuc vector in which expression can be tracked through live animal imaging. (Months 12-24)

We are working on developing the *in vivo* tracking system to efficiently follow the BMP2 transduced cells, and verify their location within the hydrogel materials. We are also currently developing a near infrared dye IR800 that will enter cells and bind to a peptide moiety known as halo tag (Promega Corp). We believe the near infrared will provide the greatest sensitivity. However, we are including preliminary data comparing three commonly used cell tracking modalities. In figure 1A, we injected varying numbers of cells transduced with an adenovirus (5000 vp/cell) possessing the DSRed, GFP, or click beetle red luciferase (CBRLuc) transgenes. As can be seen in figure 1, very little luciferase could be detected from the highest numbers of cells, and (fig 1B) none of the concentrations of cells were detected in the mice itself. Alternatively all concentrations of cells could readily be detected in the DSRed samples, and cell numbers ranging from 1×10^6 to 6×10^4 cells being detected in the animal after subcutaneous injection. We propose that introduction of the near infrared dye will allow us to detect as few as 100 cells. We propose to complete these experiments in the next quarter, and will then initiate the tracking experiments to determine both cell viability and exact location of the injected materials.

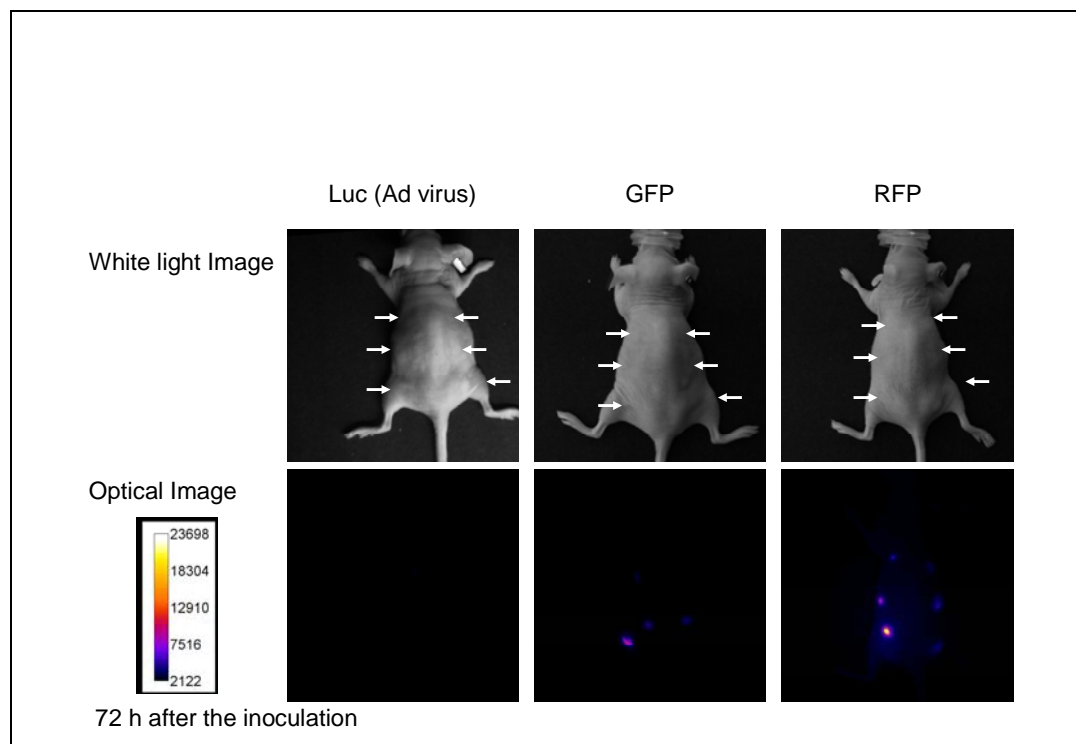
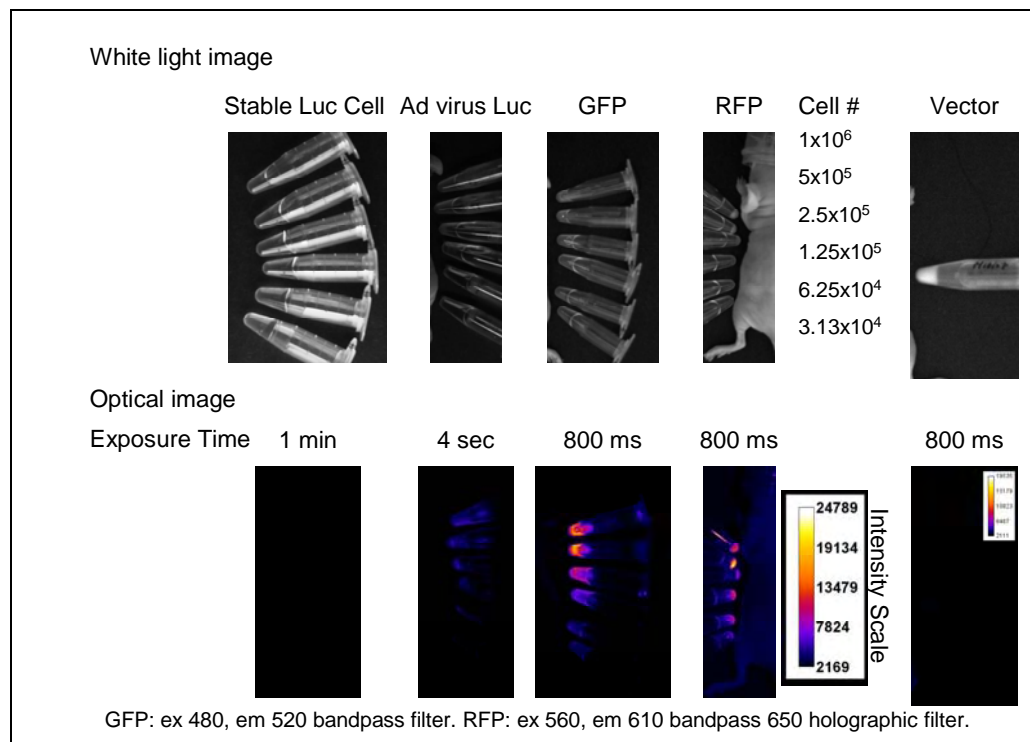


Figure 1A: Varying number of cells transduced with Ad5CBRLuc, -GFP, -DSRed, and Control “empty cassette vector” **B:** Same cells after subcutaneous injection into the mice.

With the capabilities of adding types of vectors have also been constructed to possess a report gene in the E3 region which will aid BMP2 vector tracking without worries of reduced expression associated with use of an internal ribosome entry site (IRES) or promoter interference. Our current plans are to place either dsRED or halotag in the region for cell tracking and testing.

We have currently completed all the cell culture work to confirm that the cells are maximally transduced at 7500 vp/cell both by facs analysis of the cells for the fiber gene, as well as measuring either by fluorescence cell sorting (FACs) analysis or by luciferase assays. We have also been working on repeating the animal models which are shown above. We have introduced experiments using the halo tag (Promega Corp, CA) vector which binds a substrate which we have chemically labeled with two different near infrared dyes NIR800 and NIR783. The limited autofluorescence in these wave lengths, with the longer exposure times, makes this an ideal method for tracking cell populations within the animals. In these preliminary experiments we were able to determine that the NIR800 dye (Log P value -3.75) was not readily getting into the cells, so currently we are proceeding with NIR783 (Log P value 0.40) which should be capable of diffusing into the cell. These studies are currently being done and should be completed in the next month. With completion of this work, we plan to write a manuscript outlining our comparisons of the various methods for tracking gene therapy vectors. With completion of the comparison, we will have determined the most sensitive tracking method, as well as determine the level of detection, which will be helpful in future design of the toxicology studies. Further, we will complete the additional experiments outlined in this task.

Simultaneous to these experiments in the mice, we also initiated *in vitro* studies to compare and determine the additional difficulties introduced with the hydrogel materials, in imaging the transduced cells. Towards this end, we transduced cells with luciferase and DSRred in order to determine which was more easily visible through the hydrogels. With both, there is background luminescence and fluorescence, so we ran tests to determine how much luciferin substrate was needed for the assay with cells only (ie: no hydrogel). Initially we ran serial dilutions of luciferase cell lysates, but when the signal was not strong enough, we switched to live cells, and ran serial dilutions of these, starting at 0.1×10^6 cells, reduced by half in each progressive well for 11 wells, with the 12th well filled only with buffer. The continued high background led us to attempt an assay with constant cells and increasing concentrations of luciferin starting at 300 $\mu\text{g/mL}$. We propose to terminate these studies and follow up with those using DSRred.

Thus we repeated these tests using cells transduced with Ad5DSRed. In addition, we ran the hydrogels without cells in the plate reader. The photoinitiator Eosin-Y fluoresces at the same frequency as the Ad5DSRed transduced cells, so there was a high background that could be seen on the confocal microscope. The highest concentrations of the DSRred fluoresced well above the background.

Next we wanted to determine if the hydrogel material would shield detection of the DSRred. Briefly cells were transduced with (5000 vp/cell Ad5DSRed and then either encapsulated or plated directly (Figure 2).

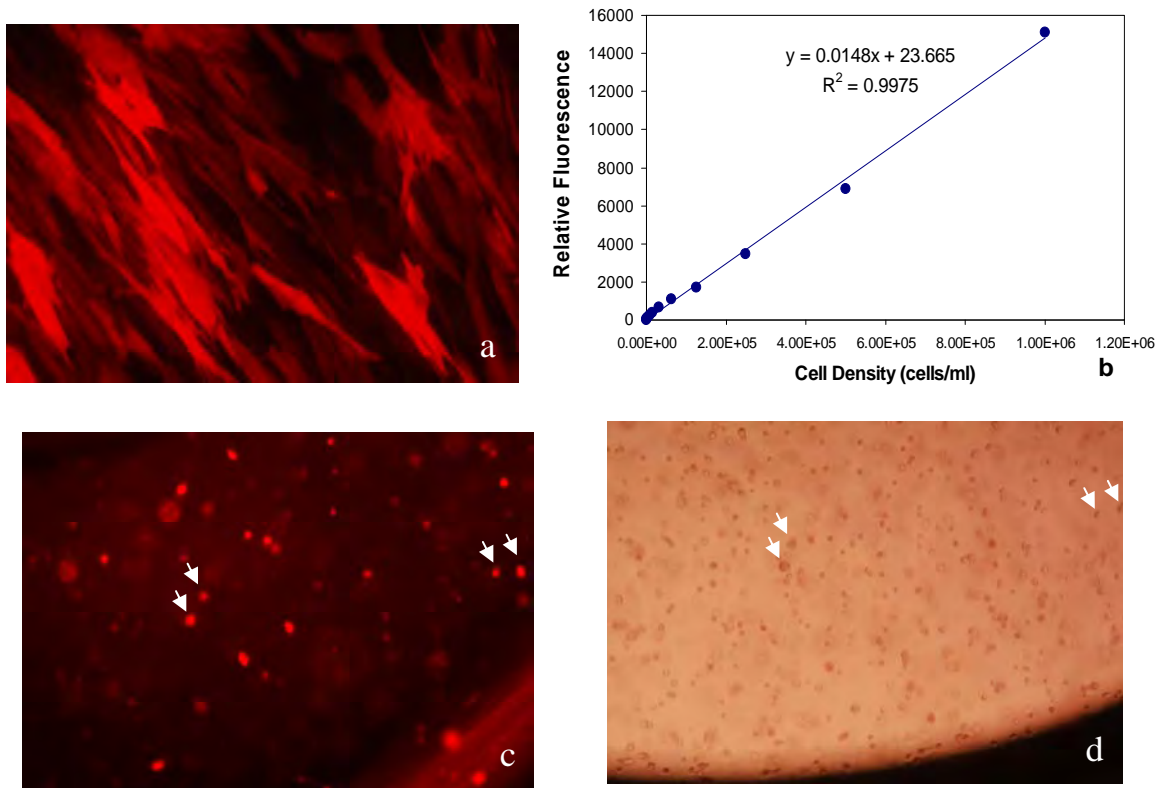


Figure 2: MRC5 cells transduced with Ad5sdRed 48 hrs in (a) monolayer (c and d) encapsulated in the PEG-DA hydrogels. (a and c) Fluorescence microscopy (d) phase contrast microscopy. (b) Fluorescence detection per cell number

Interestingly, the cells after hydrogel encapsulation lose their characteristic elongated morphology and appear more circular, demonstrating the lack of binding sites within the hydrogel materials. However, the expression appears to be detectable and somewhat equivalent to the plated cells.

We repeated these tests with DSRed to determine the sensitivity of detection through the hydrogel material. In addition, we ran the hydrogels without cells in the plate reader. The photoinitiator Eosin-Y fluoresces at the same frequency as the cells DSRed cells, so there was a high background that could be seen on the confocal microscope. The highest concentrations of the DSRed fluoresced well above the background, so with a large enough cell concentration, the background hydrogel fluorescence can be subtracted from the results. Alternatively, it is also possible to switch to a UV photoinitiator. We will continue to look at the halo tag as new data comes in. We have terminated our work using luciferase imaging. With completion of these cell culture tests we will be able to more readily implement either the DSRed or halotag animal experiments described in this task. We have completed the *in vitro* testing, and although there is background fluorescence from the photoinitiator, collection of the DSRed specific wavelength, through optical imaging has greatly alleviated this problem, and we are currently testing both direct injection and hydrogel encapsulated cells in the *in vivo* models.

We have chosen to move forward with the DSRed instead of the halo-tag due to serious issues concerning getting the dye into the cells, and through the hydrogel material in a manner that can efficiently determine the actually transgene expression. Secondly, because diffusion through the gel and cell wall is a passive continual process, the system has a background level of expression that cannot be eliminated thus significantly reducing the sensitivity and ability to quantify. With the DSRed, no additional components are required making it a very efficient tracking methodology.

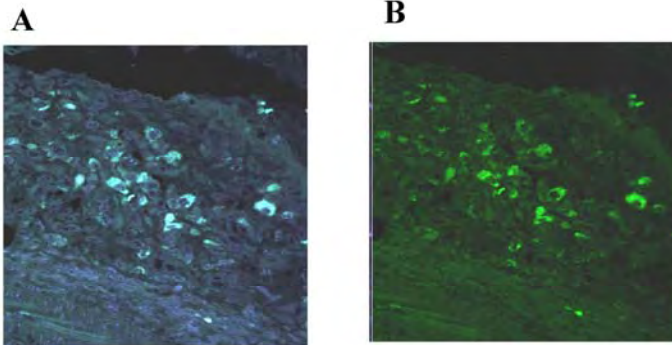
d. To track BMP2 expression *in vivo* by identifying cells undergoing BMP2 signaling through confocal imaging which follows the translocation of a Smad 1 to the nucleus. **(Months 24-48)**

We initiated these experiments earlier than proposed since the set up of imaging this *in vivo* model is a large undertaking and will require a significant amount of time to validate. Initial experiments have been done to compare and pinpoint the changes in phosphoSmad signaling in tissues receiving the Ad5BMP2 transduced cells, as compared to those receiving cells transduced with control virus. This analysis was done in tissue sections to provide preliminary data before setting up the *in vivo* imaging.

These preliminary experiments will allow us to not only pinpoint locations within the tissues to focus, but also provide us with a time frame of signaling, thus providing incite for the *in vivo* studies. Figure 3, shows immunohistochemical staining for phosphoSmad using an antibody specific to the active phosphorylated form in tissue sections taken from tissues isolated four days after injection of

the transduced cells. These initial experiments were done in wild type (C57BL/6) mice. The phoshpoSmad mice are currently constructed and are being breed to expand there numbers, as well as further characterized as to their exact phenotype.

Day 4 BMP2



Day 4 control section HM4

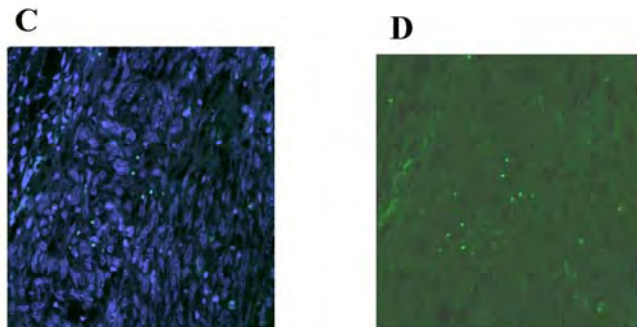


Figure 3: Immnuno-fluorescence staining on tissues isolated four days after receiving Ad5F35BMP2 transduced cells (A and B) or cells transduced with a control virus Ad4F35HM4 (C and D). Sections B and D are stained with Phospho-Smad1/5/8 antibody (1/100 dilution, Cell Signaling technology) and a secondary antibody anti-rabbit Alexa Fluor 488 conjugated. Sections A and C and stained with Phospho-Smad1/5/8 and counterstained with DAPI

- e. *Approximately 470 mice will be used in the experiments in this task. NOD\Scid 36 mice/experiment and we request three experiments, plus additional for breeding or 250 total and SMAD 1= 63 mice/experiment and we request three experiments, plus several for breeding or 220 total.*

Task 2: To design an optimal hydrogel material that will rapidly promote endochondral bone formation and be capable of removal through bone remodeling processes.

- a. *Optimize and develop a hydrogel that can be specifically degraded by osteoclasts. (Months 0-24)*

We have synthesized the peptide MGPSGPRG which has been reported to be the cathepsinK binding site (Gowen *et al*, and Hollberg *et al*), using a 431A solid-phase peptide synthesizer (Applied Biosystems, Foster City, CA), but have not yet incorporated the peptide into the hydrogel. In order to make degradable PEG, we start with PEG-DA-SMC (succinimidyl carbonate). The PEG-SMC is conjugated with our peptide in order to get PEG-PEPTIDE-PEG. So, we expect to obtain three peaks representing the completely conjugated product: PEG-PEPTIDE-PEG, incompletely conjugated

product: PEG-PEPTIDE and unconjugated product: PEG-SMC (Figure 4).

We have run GPC tests on it and the results indicate that there is still unconjugated PEG, ie: we have PEG-

Peptide or free PEG in the preparations. We have tried changing the ratio of peptide to PEG, changing the

length of conjugation time, increasing the pore size of the dialysis membrane and changing the length we dialyze the conjugation products. These have led to a higher concentration of PEG-PEPTIDE-PEG as indicated by the GPC results

Synthesis of Cathepsin K degradable PEGDA hydrogel

- Cathepsin K-sensitive sequence (CTSK):
- MGPSGPRGK
- Control sequence:
- MPGSPGGRK
- Conjugate with 3400 Da PEG-SCM

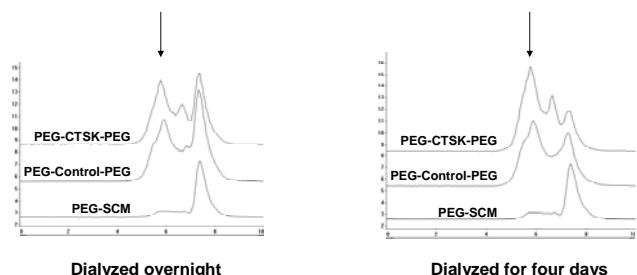
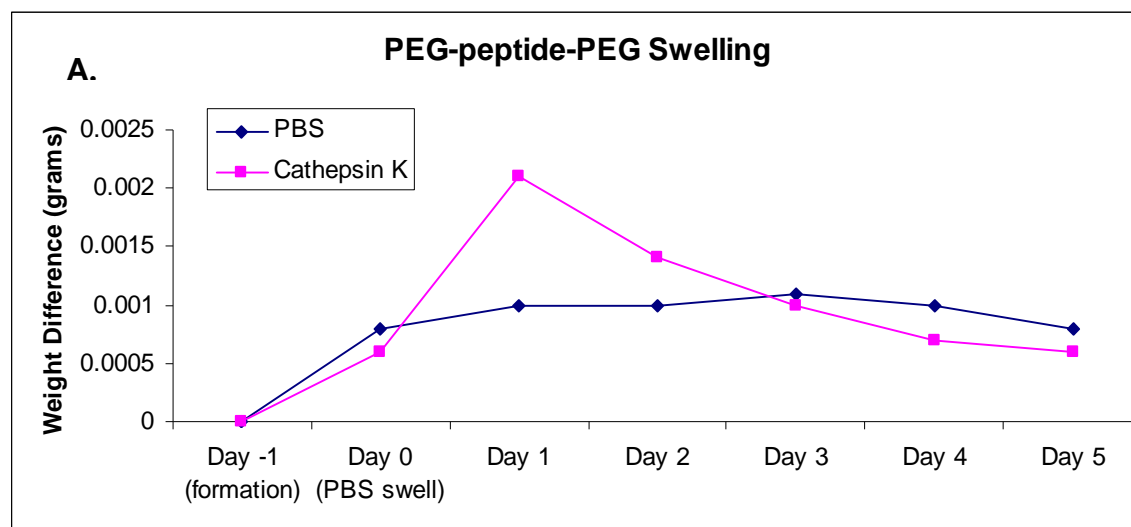


Figure 4: Results of HPLC analysis of the conjugation of peptide with the PEG-DA hydrogel.

(Figure 4). We have cathepsin K (Calbiochem; Cathepsin K, His•Tag[®], Human, Recombinant, *E. coli*) and are ready to test their degradability as described in Lee *et al*.

The next step in developing this material was to test whether the conjugation of the cathepsin K site is enough to degrade a polymerized peptide. We placed microbeads of the hydrogel in the 25 μ L cathepsin K vial (stock solution 0.2 mg/mL cathepsin K) incubated at 37°C. The PEG-peptide-PEG hydrogels (where “peptide” refers to the cathepsin K degradable peptide) were tested for swelling and degradation in PBS and cathepsin K, respectively (n=1). A swelling hydrogel typically has a logarithmic curve, like the PBS curve, where the weight of the gel increases and reaches a maximum. A degrading hydrogel will initially show an increase in weight as broken bonds allow more water in, allowing the hydrogel to swell more. Then the swollen weight will drop dramatically. Figure 5A and B shows evidence that the hydrogels are at least partly degradable. However, the results also suggest that the material cannot be completely degraded suggesting the PEG-Peptide-PEG is

limiting, or that the sites are not efficiently digested. To circumvent the latter, we are resynthesizing the peptide to include additional 3 glycines on either end to lengthen the protein region and ensure



that cathepsin K can reach it efficiently within its PEG backbone. Hopefully with the additional amino acids on the peptide site, any constraints the protease may have in binding for digestion of the site will be alleviated.

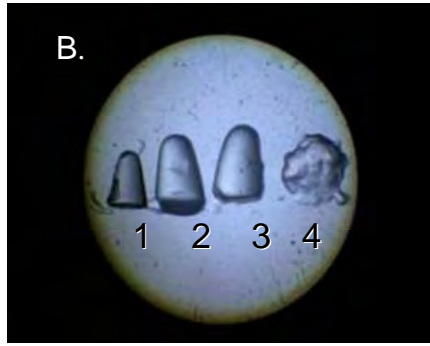


Figure 5: Swelling test of the Cathepsin K degradable peptide. **A.** Weight changes upon swelling during degradation. **B.** Hydrogels after swelling and degradation. (1) PEG-CTSK-PEG in buffer w/o proteinase K; (2) PEG-CTSK-PEG w/ 0.125 mg/ml; (3) PEG-control-PEG w/ 0.125 mg/ml; (4) PEG-CTSK-PEG w/ 0.250 mg/ml after compression.

If we observe complete degradation with the new peptide, we will then run concentration curves to

determine the minimum amount of cathepsin K required for efficient degradation. Once determined, we will run wet weight comparison experiments. First the hydrogels will be weighed and then allowed to swell in HBS with 1 mM CaCl_2 and 0.2 mg/mL sodium azide at 37°C for 24 h. Each hydrogel sample will then incubated at 37°C with HBS and the minimum concentration of cathepsin K required, 0.2 mg/mL proteinase K, 0.2 mg/mL plasmin, or no protease solution. Proteinase K will be used as a positive control for nonspecific proteolytic activity; plasmin will be used to determine selectivity of specific proteases for the cathepsin K site (negative control) and HBS without protease to demonstrate stability of the conjugated hydrogel. Degradation will then be evaluated by monitoring changes in the wet weight of hydrogels over time. The enzyme solution will be changed at 24 h intervals.

Unfortunately, the Cathepsin K, (Calbiochem; Cathepsin K, His•Tag®, Human, Recombinant, *E. coli*) is not longer commercially available. We are currently obtaining a plasmid which contains the cathepsin K cDNA and will then clone it into a plasmid vector which has the His Tag. Purification of the final protein is then readily achieved using commercial disposable column, designed to efficiently bind the His tag. Thus we will be able to generate our own cathepsin K which will significantly reduce our overall costs, since currently only non-recombinant sources are available for the protease, but are prohibitively expensive. See section III.

b. Engineer cellular binding sights within the hydrogel to determine if this improves cell viability of the transduced cells, and in turn BMP2 expression, and to tentatively enhance the migration of mesenchymal stem cells to the sight of bone formation. (Months 0-24)

We are requesting a change in the original application to include addition of a fibrin gel encapsulating the hydrogel material. This will provide an adhesion like peptide for cellular binding to the target site. We have chosen not to include these sites within the gel material since recent data suggests that it will allow entry into the gel of external cells. It appears that addition of these binding sites allows for the cells to actually bind, and open up or produce pores of the gel structure significantly altering the hydrogel properties. To offset this we are working on a gel in gel material in which the initial hydrogel will remain osteoclast degradable material, while the external gel will contain all the peptide binding sites that would allow for recruitment of progenitors and aid in establishing the initial bone. This would include the VEGD-A and D, as well as RGD binding sites (Yang *et al*). We are also testing fibrin (Fini *et al*) as previously noted in earlier reports, since this has been suggested in the literature to possess some properties that will enhance angiogenesis and osteogenesis.

c. Test addition of proteins that may enhance the BMP2 bone inductive response, such as VEGF-A or -D and compare enhancement of bone formation. (Months 24-36)

d. Test these gels in vitro. (Months 12-36)

e. Test these gels in vivo. (Months 36-48)

f. Approximately 500 mice (NOD\Scid) will be used to complete the experiments in this task. This will provide us with the 468 we need to complete the proposed experiments as well as an additional 32 for breeding stock.

Task 3: To achieve rapid bone formation by percutaneous injection of the encapsulated Ad5F35BMP2 transduced human bone marrow mesenchymal stem cells (hBM-MSCs) into the adjacent musculature of athymic rats in a model of nonunion.

- a. Once the gels have been modified to offer optimal properties for bone formation and removal, we will test these in a rat model of a critical-size defect. We will demonstrate the ability to induce bone healing in the presence of tetracycline. **(Months 24-40)**
- b. Obtain approvals through the DOD institutional review board for approval to work with the human mesenchymal stem cells. **(Months 0-12)**
 We have approval to use human mesenchymal stem cells, and are currently testing these cells for both viability and BMP2 secretion after encapsulation in the PEG-DA hydrogel. Also we have been working on developing the protocols for encapsulation of the rat fibroblasts to confirm maximum BMP2 secretion and viability. We wish to confirm that these two cell types function in the hydrogel similarly to the cells in previously published experiments. These experiments are quick and will be completed soon, thus providing us confirmation that we need to test and compare our systems in the two proposed models.
- c. Analyze the modified injectable hydrogel for optimal volume, in vivo crosslinking, design, selective degradation, and inflammatory reaction using both live animal imaging and histology. **(Months 24-48)**
- d. Bone healing will be tested both biomechanically as well as radiologically using microCT to confirm the fusion. **(Months 40-48)** Bone healing will be tested both biomechanically as well as radiologically using microCT to confirm the fusion. **(Months 40-48)**

Approvals have been obtained from Baylor College of Medicine and more recently from the Department of Defense for both the animal experiments and use of the human materials. Because we were able to complete this rapidly, we have initiated the studies using a critical defect rat model. Initial experiments using the model described by Vogelín *et al*, revealed several problems. First, we had to redesign how the plates were fitted to the bone. The rat bone is so fragile, that we were unable to place the screws, remove them, and then replace them. This ended up with the wholes being stripped and significant wobble in the plate, thus zero fixation of the bone. We have chosen to redesign this approach as outlined in figure 6. As seen in figure 6A, we first drilled the screw wholes, and removed the bone on one side of the area involved in the critical size defect. We then place the

Figure 6: Large segmental defect model in a rat. (A) Introduction of both the screw holes, to align the plate, and the initial stage of the critical size defect. (B) Placement of the plate onto the defect to fix the bone. Notice four screws in total could be placed in this model. (C) Alternative method for fixing the bone in a critical size defect rat model by creating a critical size defect in the rat fibula (x-ray).

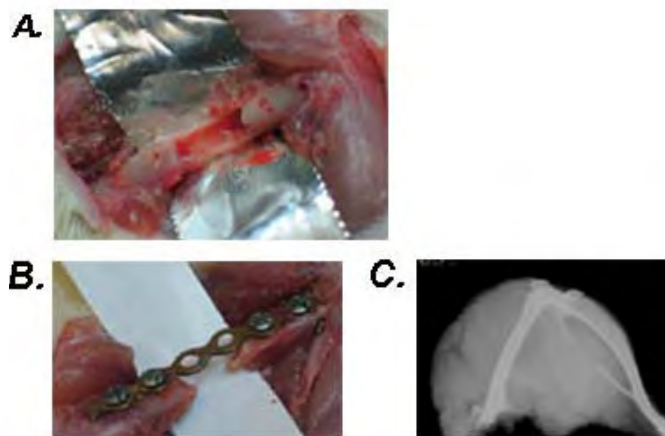


plate on the leg using four screws (figure 6B). Next we remove the remaining bridge of bone, by drilling using a Dremmel device critical size fix the

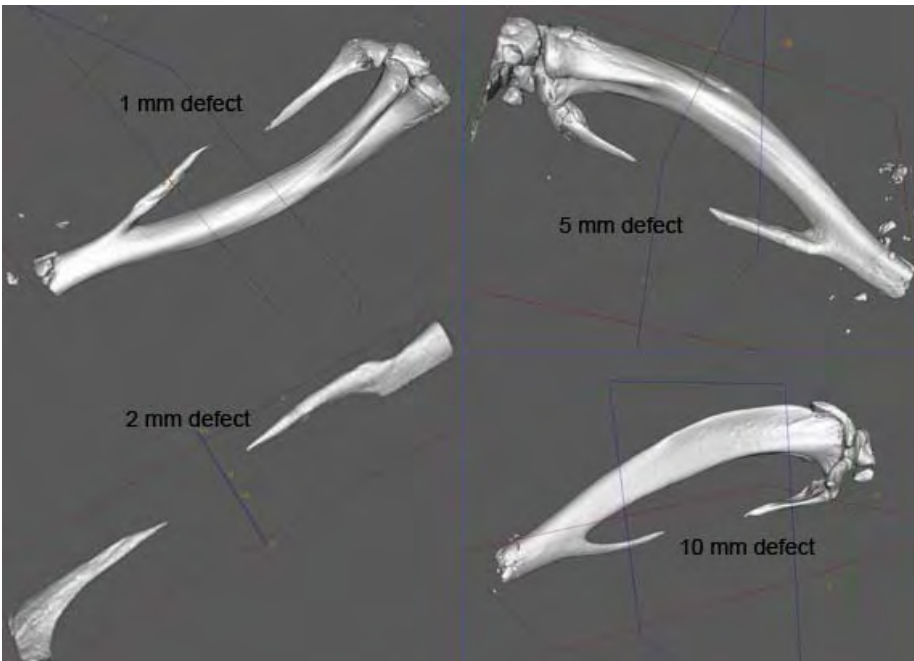
which allows us to create the defect in the rat long bone and tissue so to prevent healing. We have had good survival rates for this procedure, and the rats appear to tolerate the defects, and can easily ambulate to obtain food and water. However, in a large percentage of the animals, the plate significantly loosens, resulting in wobble or movement of the

bone, compounding or preventing any healing. Often the loss of a screw will result in fracture or shattering of the bone outside of the defect, all of which result in early euthanasia of the animals.

Thus below we propose an alternative approach, in which we create the defect in the rat fibula (Figure 6C). Briefly, this model involves introducing a critical size defect into the rat fibula. Unlike humans, the rat fibula unites with the distal tibia and does not comprise a part of the ankle joint. Recent measurements show the potential to introduce a large enough defect to be critical size. Because the tibia will remain intact, this eliminates the need for rigid fixation with additional hardware. This is much safer for the animals, which will be able to ambulate normally. Additionally if feasible, this model is much more cost effective since it requires no metal hardware. Thus the surgical times are greatly reduced as well as post-operative stress on the animals.

In this model, the rat fibula will be exposed by dissecting through the plane between the anterior and the superficial posterior muscle compartment to expose the bone. The periosteum surrounding the bone will be lifted during this procedure. Using a ronguer, specific sized deletions of critical distance will be introduced into the bone. Then, either Ad5F35BMP2, Ad5F35Empty cassette transduced cells, or the corresponding PEG-DA hydrogel encapsulated cells (Bikram *et al*) will be introduced into the defect site and healing will be monitored at weekly intervals ranging from 1-8 weeks.

In our pilot experiment, we introduced a range of defects into the fibula, and approximately 6 weeks later, euthanized the animals to evaluate bone healing. The results were extremely surprising in that all defects introduced into this bone were unable to heal. Further, the bone appeared to



undergo significant resorption (figure 7).

Figure 7: MicroCt analysis of the rat fibula 6 weeks after introduction of varying size defects. The numbers in mm represents the original size defect introduced into each sample. The samples shown are representative of n=3 samples. MicroCt analysis of the samples revealed bone healing at the boundary of the defect. Samples examined at 2 weeks appeared to have a non-mineralized central core, suggesting that the bone

had not formed over the defect boundary, whereas at 6 weeks, the end of the bone appears to be mineralized with no visible central core. As can be seen in figure 7 however, the defects appear to be substantially larger than the original defect that was introduced and the ends of the nonunion appear to be angled suggestive of substantial bone resorption rather than formation. This may be due in part to the small size of the bone, lack of substantial marrow component, and removal of the periosteum, however, it provides an extremely important model for bone healing. This model is not only reproducible, but thus provides one of the most rigorous models for inducing bone healing. We propose that introduction of the heterotopic bone at this site will not only favor formation of resorption, but will fuse into the skeletal bone to create adequate healing. Further, we propose to look determine the role removal of the periosteum is playing in either the bone resorption or the lack of bone repair.

To determine if the periosteum could be playing a critical role in induction of resorption of this bone, we analyzed histologically the bone sections removed from the long bone. Interestingly, the

fragments varied dramatically, with some lacking periosteum, suggesting it was removed during exposure for introduction of the defect; while others actually had both the periosteum as well as muscle tissue suggesting that this is not the reason for the significant resorption (data not shown). Most likely the resorption is stemming from lack of use of the bone, due to the fusion. The bone appears to resorb to a specific length from the tibial fusion site, and then stop which would be consistent with the resorption being associated with the lack of weight bearing load. In any case this model then becomes an extremely relevant and difficult model for bone healing.

As a pilot experiment we tested the ability of Ad5BMP2 transduced Wistar rat fibroblasts to heal the critical size defect. Briefly, the bone was exposed, and a 3 mm defect was introduced. Then approximately 5×10^6 Wistar rat fibroblast cell line transduced with either Ad5BMP2 or Ad5empty cassette (2500 vp/cell) in the presence of GeneJammer® (Foultier Dilling et al), were injected into the defect and the area closed with suturing. Bone formation and any potential healing was allowed to occur for 4 weeks, and then the animals were euthanized and the limbs analyzed for new bone formation using microCT.

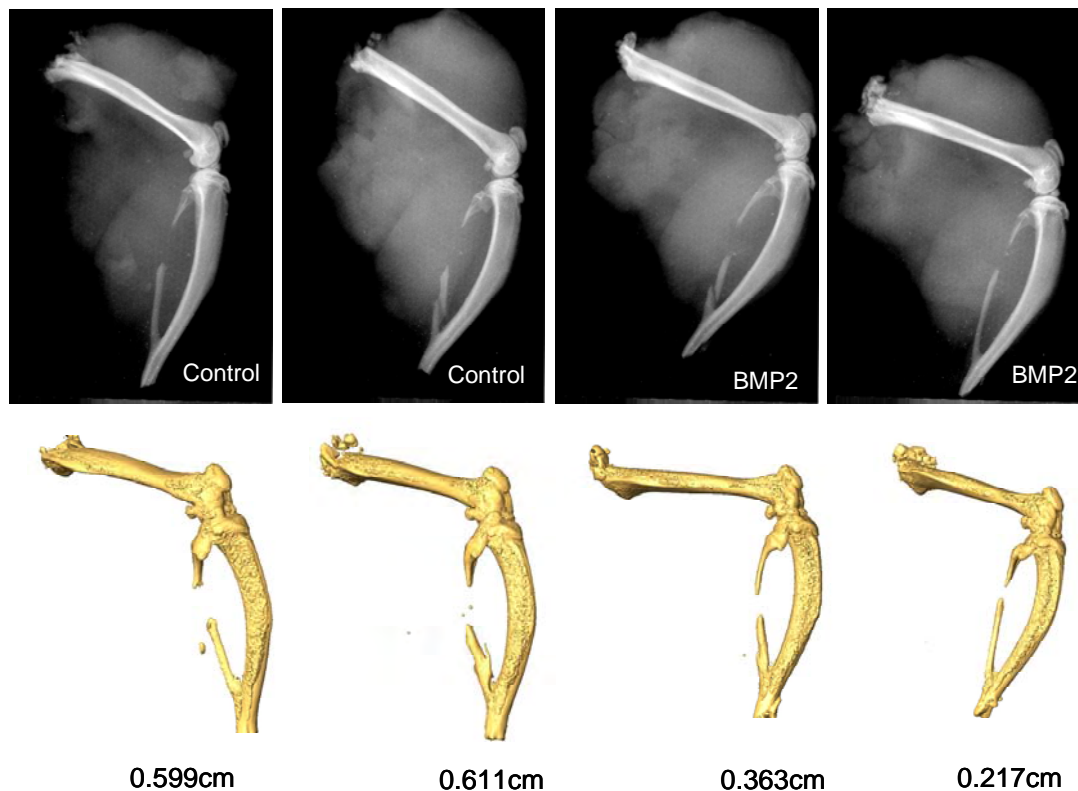


Figure 8: MicroCT of rat fibula 4 weeks after introduction of the critical size defect. In all defects, we introduced a matched rat fibroblast cell line transduced with (2500 Vp/cell) in the presence of a polyamine of either Ad5BMP2 or Ad5empty cassette control virus. The transduced cells were resuspended in PBS and then injected into critical size defect void.

As seen in figure 8, the results demonstrated that we did not get complete healing with obvious well mineralized tissues in this time frame; however, we did observe some new bone formation, as well as blocked the resorption in the remaining fibula. This was consistent for the BMP2 group whereas the groups receiving the control cells showed an enhancement in the size of the defect, stemming from the resorption.

As measured by the microCT, the defect in one of the BMP2 samples appeared to be 0-1 mm less than the initial defect introduced, suggesting again new bone formation whereas the controls were approximately 3-4 mm larger than the original defect (Figure 8). We are currently analyzing these tissues histologically to determine the extent of the new bone formation and its location, whether orthotopic or heterotopic. Further we are analyzing and quantifying the BMP2 expression from the transduced rat fibroblasts to determine the transduction efficiency. We need to confirm that our

current transduction methods are leading to adequate secretion of the BMP2 (Olmsted-Davis *et al*, and Fouletier-Dilling *et al*). These assays are simple and should be completed in a couple of weeks. Further, we will perform a second pilot experiment with limited numbers of rats, in which we look at the fate of the delivery cells, to determine if the placement in the defect void, versus the adjacent muscle alters the length of viability of the delivery cells.

Finally we are currently testing the transduction efficiency (as determined by the amount of BMP2 secreted) in the rat fibroblasts after encapsulation in the hydrogel materials. Since the health and viability of the cells can determine the amount of transgene produced, we will confirm that the cells can survive and produce transgene after encapsulation, particularly since there are not potential cellular binding sites within this material. We are currently checking both the amounts of BMP2 in the media, through ELISA and protein activity (Bikram *et al*) in the media by alkaline phosphatase assays in BMP2 responsive cell line W20-17 (Olmsted *et al*). Once we have optimized BMP2 secretion, we will encapsulate and test these cells in the critical sized defect as outlined in Figure 9. We again propose to do a gel in gel, to allow for cells recruiting to the defect void to have binding sites and be capable of undergoing chondro-osseous differentiation. The gel in gel phenomena is depicted in Figure 9 below.



Figure 9: Critical sized defect in rat fibula spanned by rod shaped hydrogel which does not contain cells (pink), and is highly crosslinked. The second gel (Red color) would possess the Ad5BMP2 transduced cells

e. Approximately 230 rats total. We request 120 NIH nude athymic rats for experiments and 108 Wistar rats to complete the experiments in this task.

Key Research Accomplishments:

Task 1: To produce high levels of BMP2 from human mesenchymal stem cells transduced Ad5F35BMP2 adenovirus in the presence of tetracycline carrying a red luciferase reporter gene.

- We have determined that DSRed is the most sensitive of the reporter modalities for detecting the cells in the hydrogel material after introduction into the mouse muscle. We have ongoing studies to compare direct injected cells to those in the hydrogel material.

Task 2: To design an optimal hydrogel material that will rapidly promote endochondral bone formation and be capable of removal through bone remodeling processes.

- We have constructed the cathepsin K protease site, and introduced it into the hydrogel material.
- We have initially tested this material and found it to be selectively degraded by cathepsin K

Task 3: To achieve rapid bone formation by percutaneous injection of the encapsulated Ad5F35BMP2 transduced human bone marrow mesenchymal stem cells (hBM-MSCs) into the adjacent musculature of athymic rats in a model of nonunion.

- We have established and set up a reproducible critical size defect model that due to the nature of the site is a tremendously challenging model of bone healing.
- We have initially tested the BMP2 transduced cells to induce bone formation and healing in this model
- Preliminary results suggest that BMP2 is capable of blocking the bone resorption in this model, as well as inducing bone healing.

Reportable Outcomes:

We have also recently published work concerning this BMP2 bone formation model in the August addition of Human Gene Therapy (see attached document). In this study, we compared bone formation in an immune competent animal to that observed in an immune incompetent mouse. We compared both the early events in bone formation (histologically) as well as bone volume during later time points after the osteoid has been established. This work is highly relevant to this application since it clearly demonstrate that bone formation occurs similarly in the two models. To further highlight the importance of this work, the journal also selected it as the cover for the August issue.

We have also been presented both a plenary poster and podium presentation at the American Society of Bone and Mineral Research 29th Annual Meeting. Both of these abstracts that were selected deal with the stem cell recruitment to the site of BMP2 bone formation as well as vessel extravasation which is required for both stem cell entry into the site as well as initial differentiation. These factors are essential preliminary data for optimizing the hydrogel materials to rapidly enhance bone formation at the target site.

The work has been presented within Baylor College of Medicine at the Annual Center for Cell and Gene Therapy Retreat. The project was both highlighted in an oral presentation as well as a poster format.

We have will present two posters at the upcoming Orthopedic Research Society Annual Meeting. The work described in the abstract highlights the work on both developing the model as well as highlighting the recent developments of the BMP2 gene therapy system in combination with the hydrogel material.

I have been asked to speak at the upcoming American Society of Gene Therapy Annual Meeting on the research in the laboratory including the development of this gene therapy system for healing critical size defects. We have also submitted an abstract for poster presentation on this work. This meeting is in Boston MA, May 28th-June 1st. My talk is currently schedule for May 31st.

Also as mentioned we are working with Clontech to develop the adenoviruses that carry both the tet activator protein as well as the tet regulated promoter-transgene cassette into the same vector. We are both working on two separate cloning approaches, with our lab being the test site for both plasmids. Once completed, Clontech has agreed to provide with the vector plasmids in exchange for the developmental testing.

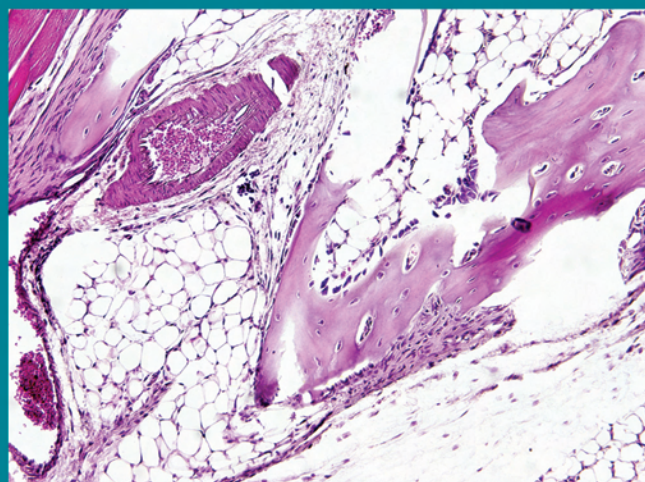
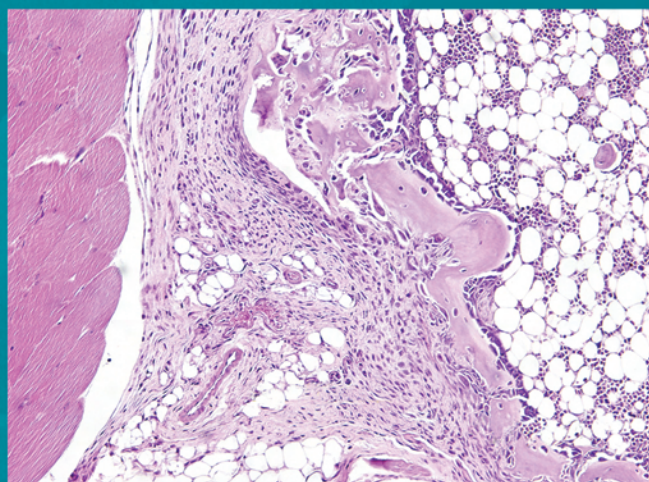
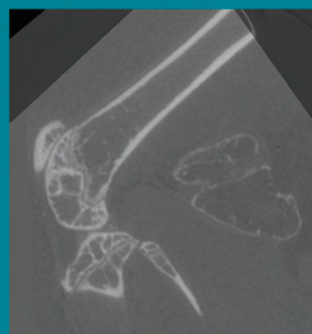
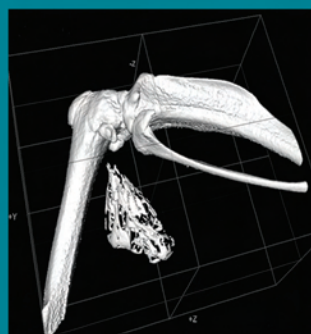
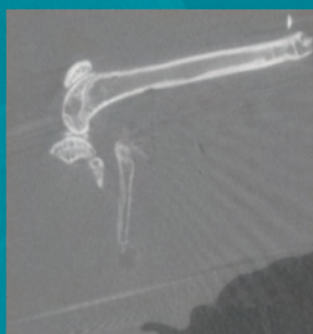
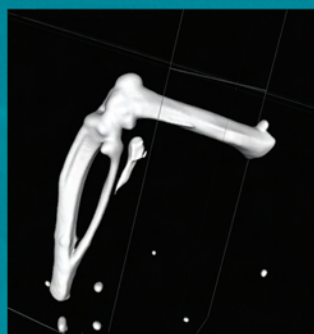
Conclusions:

We have made significant progress for this first year of the four year proposed study. In the upcoming years we hope to complete the studies described in aim 1, using the BMP2- DSRed vectors to compare temporal and spatial expression of BMP2 on endochondral bone formation. We also hope to complete the initial *in vitro* developmental phase of the osteoclast degradable hydrogel material. Finally we have not only established a challenging model of non-union critical size defects in rats, but also have preliminary data that BMP2 is capable of healing or producing bone under these circumstances. We believe in the upcoming year that we will further optimize this system to obtain the rapid and complete healing of the defect. Further, we will determine if this is due to heterotopic bone formation fusing into the orthotopic, or stimulation of the orthotopic bone by BMP2 to induce healing. Thus we have considerable challenges in the second year of this proposal, but have enough preliminary data from the first year to suggest success in our endeavors.

References:

1. Gowen, M., et al. (1999). Cathepsin K knockout mice develop osteopetrosis due to a deficit in matrix degradation but not demineralization. *J Bone Miner Res* 14: 1654-1663.
2. Hollberg, K., Nordahl, J., Hultenby, K., Mengarelli-Widholm, S., Andersson, G., and Reinholt, F. P. (2005). Polarization and secretion of cathepsin K precede tartrate-resistant acid phosphatase secretion to the ruffled border area during the activation of matrix-resorbing clasts. *J Bone Miner Metab* 23: 441-449.
3. Lee, S. H., Miller, J. S., Moon, J. J., and West, J. L. (2005). Proteolytically degradable hydrogels with a fluorogenic substrate for studies of cellular proteolytic activity and migration. *Biotechnol Prog* 21: 1736-1741.
4. Yang, F., Williams, C. G., Wang, D. A., Lee, H., Manson, P. N., and Elisseeff, J. (2005). The effect of incorporating RGD adhesive peptide in polyethylene glycol diacrylate hydrogel on osteogenesis of bone marrow stromal cells. *Biomaterials* 26: 5991-5998.
5. Fini, M., et al. (2005). The healing of confined critical size cancellous defects in the presence of silk fibroin hydrogel. *Biomaterials* 26: 3527-3536.
6. Vogelin E, Jones, NF, Huang JI, Brekke JH, Lieberman, JR (2005) Healing Critical-Sized Defect in the Rat Femur with Use of a Vascularized Periosteal Flap, a Biodegradable Matrix, and Bone Morphogenetic Protein. *J Bone Joint Surg* 87-A(6) 1323-1331.
7. Foulletier-Dilling, CM. et al. (2005). Novel compound enables high-level adenovirus transduction in the absence of an adenovirus-specific receptor. *Hum Gene Ther* 16: 1287-1297.
8. Foulletier-Dilling CM, Gannon F, Olmsted-Davis EA, Lazard Z, Heggeness MH, Shafer JA, Hipp JA, and A.R. Davis. (2007) Efficient and Rapid Osteoinduction in an Immune Competent Host. *Hum Gene Ther* 18(8):733-45 (Fast Track publication and Cover).
9. Olmsted-Davis, EA, et al. (2002). Use of a chimeric adenovirus vector enhances BMP2 production and bone formation. *Hum Gene Ther* 13: 1337-1347.
10. Bikram M, Foulletier-Dilling CM, Hipp JA, Gannon F, Davis AR, Olmsted-Davis EA, and West JL (2007) Endochondral Bone Formation from Hydrogel Carriers Loaded with BMP2-Transduced Cells. *Ann Biomed Eng.* 35(5):796-807.
11. Olmsted, EA. et al. (2001). Adenovirus-mediated BMP2 expression in human bone marrow stromal cells. *J Cell Biochem* 82: 11-21.

Human Gene Therapy



Mary Ann Liebert, Inc.  publishers

Human Gene Therapy

VOLUME 18, NUMBER 8, AUGUST 2007



LIEBERT

Efficient and Rapid Osteoinduction in an Immune-Competent Host

CHRISTINE M. FOULETIER-DILLING,¹ FRANCIS H. GANNON,^{1–3}
ELIZABETH A. OLMSTED-DAVIS,^{1,2,4} ZAWAUNYKA LAZARD,¹ MICHAEL H. HEGGENESS,²
JESSICA A. SHAFER,^{1,4} JOHN A. HIPPI,² and ALAN R. DAVIS^{1,2,4}

ABSTRACT

Osteoinductive systems to induce targeted rapid bone formation hold clinical promise, but development of technologies for clinical use that must be tested in animal models is often a difficult challenge. We previously demonstrated that implantation of human cells transduced with Ad5F35BMP2 to express high levels of bone morphogenetic protein-2 (BMP2) resulted in rapid bone formation at targeted sites. Inclusion of human cells in this model precluded us from testing this system in an immune-competent animal model, thus limiting information about the efficacy of this approach. Here, for the first time we demonstrate the similarity between BMP2-induced endochondral bone formation in a system using human cells in an immune-incompetent mouse and a murine cell-based BMP2 gene therapy system in immune-competent animals. In both cases the delivery cells are rapidly cleared, within 5 days, and in neither case do they appear to contribute to any of the structures forming in the tissues. Endochondral bone formation progressed through a highly ordered series of stages that were both morphologically and temporally indistinguishable between the two models. Even long-term analysis of the heterotopic bone demonstrated similar bone volumes and the eventual remodeling to form similar structures. The results suggest that the ability of BMP2 to rapidly induce bone formation overrides contributions from either immune status or the nature of delivery cells.

OVERVIEW SUMMARY

The rapid osteoinductive nature of BMP2 makes this an ideal candidate for use in cell-based gene therapy approaches, because long-term expression is not required. Progression through endochondral bone formation to vascularized bone occurs even in the presence of substantial clearing of the transduced cells. In these systems the transduced cells are not required to contribute to the final bone structures, and thus potential alteration of cellular function through viral transduction is not a concern. However, translation into the clinic has been slowed by difficulty in developing a human system that can be readily tested in animal models. If human cells are used, the choice of animal models becomes limited to immune-compromised animals. Here we compared endochondral bone formation in two such gene therapy systems with consistent BMP2 expression to determine the impact on efficacy of the various cell types and immune background.

INTRODUCTION

THE ABILITY TO INDUCE bone formation via gene therapy is a desirable goal for a wide range of clinical conditions affecting the skeleton. Thus there are numerous studies seeking to develop both virus- and nonvirus-based gene therapy systems that can introduce genes encoding osteogenic factors that can lead to rapid bone formation. These systems vary widely in the osteoinductive component employed, delivery strategies, and efficacy.

One of the best studied families of osteoinductive proteins are the bone morphogenetic proteins (BMPs). The original members of this family were identified from bone matrix by their ability to induce “*de novo*” bone formation in skeletal muscle (Urist, 1965; Wozney *et al.*, 1988). Since the time of this original finding, recombinant BMP2 protein has been introduced into the clinic for the enhancement of spine fusion. BMP2 is often used in conjunction with, or as an alternative to, bone graft materials. However, there are difficulties with delivery of

¹Center for Cell and Gene Therapy, ²Department of Orthopedic Surgery, ³Department of Pathology, and ⁴Department of Pediatrics, Baylor College of Medicine, Houston, TX 77030.

the recombinant protein. It is extremely labile and must be combined with a collagen carrier in order to maintain a high enough concentration locally to induce bone formation (Bonadio *et al.*, 1999). Uludag *et al.* (2001) have shown that the injection of BMP2 alone without a carrier to retain it at the target site results in little or no bone formation. Reports describe significant acute inflammation associated with this treatment, which led to detrimental side effects in many cases (Christ *et al.*, 1997; Alden *et al.*, 1999; Molinier-Frenkel *et al.*, 2002).

The use of cell and gene therapy presents an alternative strategy for BMP delivery. Several studies have attempted to directly administer the BMP2 gene via viral vectors, with limited success (Musgrave *et al.*, 1999). In all cases, this system yielded little to no bone formation, leaving investigators to speculate on whether additional osteoinductive components are necessary for endochondral bone formation. One of the most studied additions to this system was inclusion of an osteoprogenitor or mesenchymal stem cell as the delivery cell for the BMP2 (Lieberman *et al.*, 1998; Gazit *et al.*, 1999; Lee *et al.*, 2002; Niyibizi *et al.*, 2004). However, the results of this work are somewhat conflicting, in that most studies reported no engraftment of the cells into the endochondral bone, yet it is widely believed that the cells are necessary for coordinating bone formation.

Weiss *et al.* (2006) suggested the inclusion of vascular endothelial growth factor, in combination with the BMPs, as a means of enhancing the reaction. However, our studies show that the transduction efficiency of the delivery cells for optimal BMP2 production is the key parameter in determining the extent of bone formation (Olmsted *et al.*, 2001; Olmsted-Davis *et al.*, 2002). We demonstrated that efficient transduction of cells to express BMP2 could induce rapid endochondral bone formation (Gugala *et al.*, 2003) and was independent of the cell type transduced. But interpretation of this work and translation into the clinic have been complicated by the fact that the murine model was immune compromised, and thus may be providing a "unique" environment for the virally transduced delivery cells to survive and function. The requirement to use human cells and an immune-compromised animal model comes from the restriction of the chimeric virus to human cells, with most murine cells completely lacking its CD46 receptor (Mallam *et al.*, 2004; Fouletier-Dilling *et al.*, 2005).

To circumvent this issue we developed a cell-based gene therapy system in which autologous murine cells could be readily transduced to express BMP2, which resulted in rapid endochondral bone formation when cells were delivered to normal mice (Fouletier-Dilling *et al.*, 2005). This system employs a polyamine compound known as GeneJammer (Stratagene, La Jolla, CA), which provides a novel entry route for the virus, thus bypassing the need for a specific receptor. We have shown this to be effective at transducing a variety of animal cells as well (Bosch *et al.*, 2006).

Here we present a detailed comparison of the two gene therapy models: for the ability of the transduced cells to produce BMP2 long term *in vivo*, to recapitulate all the stages of endochondral bone formation, and to retain the newly formed bone at steady state levels, long term at a targeted location. In both approaches, we observed rapid endochondral bone formation that appears to be independent of immune background. We have demonstrated that BMP2 production is sufficient in both sys-

tems to induce the entire endochondral bone formation cascade following injection of the transduced cells. This bone production proceeds from new vessel formation, with associated inflammation, to rapid cell expansion and chondrogenesis, within 4–5 days of induction. Mineralized bone formation was observed in the tissues, independent of the model, within 7 days of induction. Within 2 weeks of the initial induction bone formation appeared to plateau, then significantly decreased to a steady state level. Comparison of heterotopic bones at 2 and 4 weeks suggested that remodeling into a well-mineralized exterior, with a hollow interior reminiscent of skeletal bone, had taken place.

MATERIALS AND METHODS

Cell culture

A murine osteoblast cell line (MC3T3-E1) and a human fibroblast cell line (MRC-5) were obtained from the American Type Culture Collection (Manassas, VA) and propagated in α -minimum essential medium (α -MEM) and Dulbecco's modified Eagle's medium (DMEM), respectively. Neither cell type is able to induce bone formation before transduction. The cell lines were supplemented with 10% fetal bovine serum (HyClone, Logan, UT), penicillin (100 units/ml), streptomycin (100 μ g/ml), and amphotericin B (0.25 μ g/ml) (Invitrogen Life Technologies, Gaithersburg, MD). A murine stromal cell line (W20-17) (a gift from Genetics Institute, Cambridge, MA) was propagated as described by Thies *et al.* (1992). Briefly, the cells were grown in DMEM supplemented as described above and cultured at a subconfluent density in order to maintain the phenotype. All cell types were grown at 37°C and 5% CO₂ in humidified air.

Transduction of cells with adenovirus in the presence of GeneJammer

Adenoviruses. Replication-defective E1,E3-deleted first-generation human type 5 adenovirus (Ad5) and/or modified forms in which the human adenovirus type 35 (Ad5F35) fiber protein has been substituted for Ad5 fiber were constructed to carry cDNAs for BMP2 in the E1 region of the virus (Olmsted *et al.*, 2001). The viral particle (VP)-to-plaque-forming unit (PFU) ratios were as follows: 55, 76, 200, and 111 for Ad5BMP2, Ad5F35BMP2, Ad5-empty, and Ad5F35HM4, respectively, and all viruses were shown to be negative for replication-competent adenovirus. We have previously demonstrated the efficient uptake of Ad5BMP2 in the presence of GeneJammer (Fouletier-Dilling *et al.*, 2005) whereas, in contrast, viral transduction using Ad5F35BMP2 in human cells does not require any additional agents (Olmsted-Davis *et al.*, 2002). Although the GeneJammer compound does enhance the uptake of Ad5F35BMP2 in mouse cells, most of our comparison data had been gathered with Ad5BMP2, which has the identical transgene cassette; thus, to avoid any unnecessary duplication, we continued to use the two separate viruses.

Cell transduction. MC3T3 cells (1×10^6) were transduced with Ad5BMP2 at a viral concentration of 5000 VP/cell with 1.2% GeneJammer. This is a critical procedure for the produc-

tion of bone in C57BL/6 mice, as MC3T3 cells lack the receptor for Ad5, the coxsackievirus–adenovirus receptor (CAR), and therefore GeneJammer is used to efficiently transduce these cells (Fouletier-Dilling *et al.*, 2005). The polyamine compound was used at a concentration previously determined (Fouletier-Dilling *et al.*, 2005). Briefly, 15 μ l of GeneJammer or phosphate-buffered saline (PBS) was added to 500 μ l of α -MEM without supplements and incubated for 10 min at room temperature. The virus was then added at the indicated concentrations and the mixture was further incubated for 10 min at room temperature. This virus–GeneJammer mixture was added to approximately 1×10^6 cells along with 750 μ l of α -MEM supplemented with 10% fetal bovine serum (FBS) and antibiotics–antimycotics. The cells were incubated at 37°C for 4 hr and then the mixture was diluted with 3 ml of fresh medium containing FBS. MRC-5 cells (human diploid embryonic lung fibroblasts) were transduced as previously described (Davis *et al.*, 2000) with Ad5F35BMP2 at a viral concentration of 2500 VP/cell. Ad5F35BMP2 was used only for transduction of human cells.

Quantification of BMP2

BMP2 protein was measured in culture supernatant taken from MC3T3 cells 72 hr after transduction with various concentrations of Ad5BMP2 in the presence of GeneJammer. Similarly, BMP2 protein was measured in culture supernatant taken from MRC-5 cells 72 hr after transduction with various concentrations of Ad5F35BMP2. Briefly, 10^6 cells were transduced as described above and culture supernatant was collected and assayed with a BMP-2 Quantikine ELISA kit from R&D Systems (Minneapolis, MN).

Alkaline phosphatase assay

W20-17 cells were assayed for alkaline phosphatase activity 3 days, after addition of culture supernatant from either Ad5BMP2, Ad5-empty, Ad5F35BMP2, Ad5F35HM4, or medium alone, using a chemiluminescence procedure (Olmsted *et al.*, 2001). Cellular alkaline phosphatase was extracted by three freeze–thaw cycles in a 100- μ M/cm² concentration of 25 mM Tris-HCl (pH 8.0) and 0.5% Triton X-100 and the activity was then measured by addition of CSPD substrate (ready-to-use) with Sapphire-II enhancer (Tropix; Applied Biosystems, Foster City, CA) to the samples. The light output from each sample was integrated for 10 sec, after a 2-sec delay, with a luminometer (TD-20/20; Turner BioSystems, Sunnyvale, CA). Alkaline phosphatase levels were recorded in relative luminescence units (RLU) and normalized to protein content with the bicinchoninic acid (BCA) assay, using bovine serum albumin to derive a standard curve. Data are presented as percent induction relative to that of unstimulated basal control cells. Statistical analysis was performed as described previously. Briefly, all data were taken in triplicate and reported as mean and standard deviation. A Student *t* test with 95% confidence interval ($p < 0.05$) was done between the untreated control and each experimental condition.

Heterotopic bone assay

MC3T3 cells were transduced in the presence of GeneJammer with Ad5BMP2 (5000 VP/cell) or Ad5-empty (5000

VP/cell), which is a control adenovirus type 5 vector that lacks a transgene in the E1-deleted region. Briefly, cells were removed with trypsin, resuspended at a concentration of 5×10^6 cells per 100 μ l of PBS, and then delivered by intramuscular injection into the hind limb quadriceps muscle of C57BL/6 mice (three animals per group). MRC-5 cells were transduced with Ad5F35BMP2 (2500 VP/cell) or Ad5F35HM4, which is a control adenovirus lacking a transgene cassette, and then injected into the hind limb quadriceps muscle of nonobese diabetic/severely compromised immunodeficient (NOD/SCID) mice ($n = 6$). Animals were killed after injection of the transduced cells, at daily intervals for the first week, and then at weekly intervals (2–4 weeks) for long-term studies. At appropriate times, hind limbs were harvested and placed in formalin. All animal studies were performed in accordance with standards of the Baylor College of Medicine (Houston, TX), Department of Comparative Medicine after review and approval of the protocol by the Institutional Animal Care and Use Committee (IACUC).

Histological analysis and staining analysis

Mouse hind limbs were formalin fixed, decalcified, and divided in half longitudinally to expose the internal tissues and then both halves of the tissue were embedded into a single paraffin block. The tissues were oriented so that the internal areas were exposed to the outside of the paraffin block, allowing the tissue to be sectioned from the inside out. Serial sections (5 μ m) were prepared that encompassed the whole hind limb reactive site (approximately 10–15 sections per tissue specimen depending on the type of transduced cells the tissue received). The reactive area within the tissues was consistently larger in samples undergoing bone formation than in adjacent control tissues. We then performed hematoxylin and eosin staining on every fifth slide to locate the central region containing either delivery cells or newly forming endochondral bone. Once this site was located, serial unstained slides were used for immunohistochemical staining. All tissue images presented in this paper were within the central region of the reaction, and representative of the other sections found in the tissues. Immunohistochemistry was performed with a Homo-Mouse Poly-HRP IHC detection kit (ImmunoVision Technologies, Brisbane, CA), according to the manufacturer's instructions for the following antibodies: hexon antibody (Clontech, Palo Alto, CA) and human mitochondria (Chemicon International/Millipore, Temecula, CA). All sections were analyzed by light microscopy.

Microcomputed tomography

Specimens isolated at 2, 3, and 4 weeks were scanned with a microcomputed tomography (MicroCT) system (eXplore Locus SP; GE Healthcare, London, ON, Canada) at 14- μ m resolution. Bone density was determined with a density calibration phantom. Three-dimensional reconstructions of the region injected with BMP2-producing cells were generated to identify regions of heterotopic ossification. The volume of heterotopic mineralized tissue was then calculated with the use of the quantitative bone analysis software provided with the MicroCT system. For this analysis, any tissue with a hydroxyapatite density greater than 0.26 g/cm³ was considered mineralized tissue. The

total volume of heterotopic mineralized tissue was measured for the right and left hind limbs, and the difference in values between C57BL/6 and NOD/SCID mice was assessed by standard *t* test analysis.

RESULTS

BMP2 expression and activity

For comparison, the two cell-based gene therapy systems were evaluated for their ability to secrete BMP2, so that in future analysis both systems would be producing equivalent amounts of BMP2. Thus, BMP2 expression was measured by quantifying the amount of protein secreted into the culture supernatant after transduction of the cells with the respective adenoviruses at various multiplicities of infection (MOIs). Culture supernatants were collected 72 hr after the initial transduction and BMP2 was quantified by an enzyme-linked immunosorbent assay (ELISA). MOIs were adjusted so that the expression levels of BMP2 between the MC3T3 cells transduced with Ad5BMP2, and the MRC-5 cells transduced with Ad5F35BMP2, were the same (Fig. 1A). On the basis of these findings, all other subsequent studies were done with these doses so as to have comparable expression of BMP2.

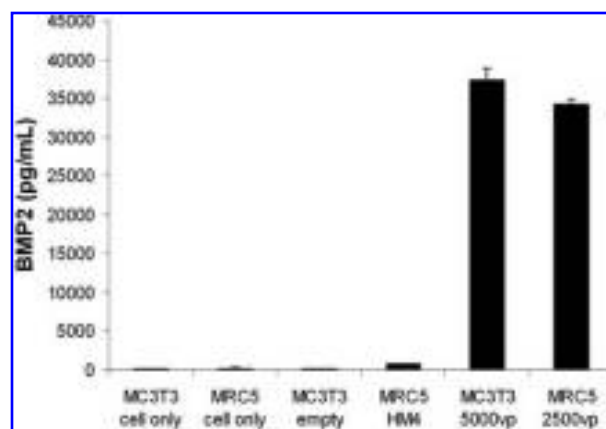
We next determined the functional activity of BMP2 protein, using a W20-17 cell-based assay (Thies *et al.*, 1992), which measures the induction of alkaline phosphatase in response to active BMP2. In this assay, the murine bone marrow cell line W20-17 was exposed to culture supernatant from MC3T3 cells or MRC-5 cells that had been transduced, respectively, with Ad5BMP2 at a concentration of 5000 VP/cell or Ad5F35BMP2 at a concentration of 2500 VP/cell. Culture supernatants from

MC3T3 and MRC-5 cells transduced with control viruses were also included to verify that the W20-17 response was specific to BMP2. Cell lysates were assayed for alkaline phosphatase activity approximately 3 days after addition of the tentative BMP2-containing supernatant. In all cases in which cells were transduced with AdBMP2 viruses, the cells secreted active BMP2, with no significant differences (*p* value is 0.6985) (Fig. 1B), whereas supernatants from cells transduced with control viruses did not induce alkaline phosphatase activity.

Absence of delivery cells by day 6

With establishment of the transduction criteria essential for each system to make equivalent active BMP2, these transduced cells were then tested for engraftment potential in the corresponding mouse models. The Ad5BMP2 model was developed to efficiently transduce autologous C57BL/6 cells for induction of bone in an immune-competent setting (Fouletier-Dilling *et al.*, 2005); we next measured engraftment of these cells into the site of bone formation and compared this with Ad5F35BMP2-transduced human cells delivered to immune-incompetent NOD/SCID mice. These human fibroblast cells (MRC-5) are diploid embryonic lung fibroblasts but are not osteogenic or derived from marrow stromal cells (MSCs). Even though MC3T3 cells are considered to be "osteoblastic," no bone formation was ever observed when using nontransduced cells or cells transduced with control vector. Because both cell types possess adenoviral antigens as a result of transduction with first-generation adenoviral vectors, we were interested in determining whether the human cells would have similar survival rates in NOD/SCID mice, which lack the lymphocytic arm of the immune system, as compared with the cells delivered to wild-type mice.

A



B

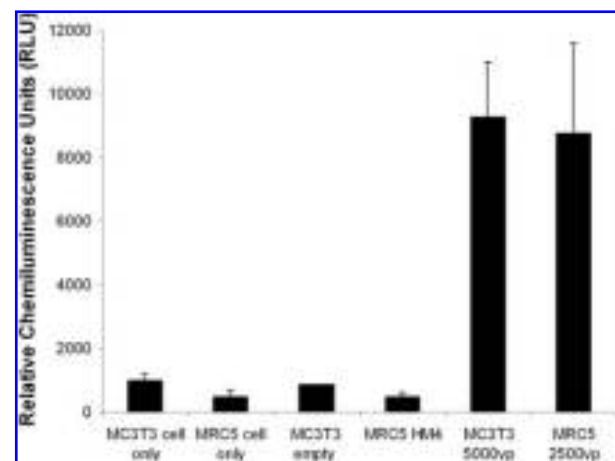


FIG. 1. Quantification of BMP2 *in vitro* (A) and activity of BMP2 (B). (A) The quantity of BMP2 was measured in culture supernatants taken from MC3T3 cells transduced with Ad5BMP2 (5000 VP/cell) and MRC-5 cells transduced with Ad5F35BMP2 (2500 VP/cell), using a Quantikine assay (R&D Systems). The concentration of BMP2 was extrapolated by comparison with a standard curve based on known concentrations of recombinant BMP2. BMP2 concentrations in the supernatant are reported as picograms per milliliter ($n = 3$). $p > 0.5$ (Student *t* test). (B) BMP2 activity, measured in culture supernatants taken from MC3T3 cells transduced with Ad5BMP2 (5000 VP/cell) and MRC-5 cells transduced with Ad5F35BMP2 (2500 VP/cell), was determined by measuring the increase in alkaline phosphatase activity in W20-17 cells 72 hr after exposure. Alkaline phosphatase activity is depicted as average relative chemiluminescence units (RLU), where $n = 3$. Columns and error bars represent means and standard deviation, respectively, for $n = 3$ experiments. $p > 0.5$ (Student *t* test).

The cells were tracked by two different systems. In the NOD/SCID (immune-incompetent) model, human cells were detected by immunohistochemical staining for expression of a protein specific to human mitochondria. We observed positive staining for human cells in tissues isolated from 1 to 5 days after induction (Fig. 2A), but human cells were completely absent by day 6 after their initial injection into muscle. In the C57BL/6 (immune-competent) model, we looked for expression of the hexon protein, the largest and most abundant of the structural proteins in the icosahedral adenoviral capsid, by immunohistochemistry as a means of locating the transduced cells. As seen in Fig. 2B, transduced cells were still present on day 6 after induction, but had not engrafted into any tissue structures associated with the newly forming bone. By 7 days postinduction, the transduced cells were completely absent in all tissue sections encompassing the reaction site. These results demonstrate that the transduced cells are cleared before bone formation. However, in all cases the cells did not appear to be associated with any of the newly forming cartilage and bone. Interestingly, the cells were cleared at the same rate in both systems, seemingly independent of the immune status of the animal.

Stage-by-stage comparison of bone formation in immune-competent and immune-deficient mouse models

We have characterized, by immunohistochemical phenotyping and cell tracking, the initial stages of endochondral bone formation in the NOD/SCID model (Olmsted-Davis *et al.*, 2007; Shafer *et al.*, 2007). These stages are extremely reproducible and include the appearance of brown adipocytes on days 1–2, new vessels on days 3–4, cartilage on days 4–6, and bone on days 6–8. These previous studies have linked the early mesenchymal precursors for chondrocytes and osteoblasts to be of myelomonocytic origin (Shafer *et al.*, 2007).

Here we compared these stages of endochondral bone formation between the two mouse models, given that both systems are capable of producing equivalent functional BMP2, as well as with control mice that received cells transduced with an empty cassette vector. The emphasis was on detection of any differences in the progression of endochondral bone formation, including temporal changes that may result from the difference in immunological background of the animals. Figure 3 shows resultant photomicrographs from the immune-competent model (C57BL/6), the immune-incompetent model (NOD/SCID), and the control mice on days 2, 4, 6, and 7. The images are representative of the reaction within the tissues for each of the days. As can be seen in Fig. 3, day 2, the sections look similar, with both delivery cells and visible inflammation present in the tissues regardless of whether the cells were expressing BMP2. However, by 4 days after the initial injection, the experimental sections for both models no longer match the control sections. Tissues receiving cells transduced to express BMP2 showed a significant increase in the number of cells within the tissues. Our previous studies have shown these cells to be myelomonocytic precursors both migrating into the tissues as well as proliferating to form new cartilage (Shafer *et al.*, 2007). Alternatively, the inflammatory response is essentially gone by day 4 in the control sections. Both transduced

cells as well as host-derived cells are greatly reduced in volume compared with the previous days (see Fig. 3) and these results confirm earlier data showing the disappearance of delivery cells in both systems (Fig. 2). The cartilage is well established and similar in the experimental sections from both models on day 6; however, the control section demonstrates a complete absence of both inflammatory cells and injected cells. By day 7 newly formed bone is observed in both models that received BMP2-transduced cells, suggesting that the presence of a complete immune system did not reduce the rapid nature of endochondral bone formation previously reported in the immune-competent model.

Long-term bone expression

Although endochondral bone formation during the first 7 days was histologically similar in both systems, we wanted to compare long-term bone formation, and/or retention. Figure 4 represents the hematoxylin and eosin-stained photomicrographs taken of tissues isolated from the immune-incompetent model (NOD/SCID) and immune-competent model (C57BL/6) 2, 3, and 4 weeks after injection of BMP2-producing cells. The results of histological analysis of the sections are dramatically different between the 2- and 4-week time points but remain similar between the two systems. As expected, the bone appears to be remodeling into a more hollow structure, but surprisingly, a large amount of fat cells are appearing over time in the central compartment or presumptive marrow cavity of this tissue.

Microcomputed tomographic analysis was performed on tissues ($n = 6$) isolated 2, 3, and 4 weeks after induction of bone formation to compare total bone volume between the two model systems (Fig. 5A). The results show similar bone volume at all time periods, with no significant difference between the two systems; however, there was a significant decrease in the overall bone volume in both systems when samples were compared temporally (Fig. 5A). The bone volume peaked at 2 weeks and decreased significantly by 4 weeks in both models (Fig. 5A). Heterotopic bone is apparent in all samples, regardless of the model. Three-dimensional reconstructions of heterotopic bone from representative NOD/SCID and C57BL/6 tissue samples are shown in Fig. 5B. Two-dimensional cross-sectional analyses of the three-dimensional reconstruction show thicker bone that is less well mineralized in both NOD/SCID and C57BL/6 tissue samples at 2 weeks, and becomes much thinner and more well mineralized by 4 weeks. This change in overall bone volume may reflect both the remodeling of the presumptive marrow cavity as well as the lack of weight-bearing forces on the heterotopic bone.

Dose response

We next measured dose response for bone formation via the injection of genetically modified cells. Accordingly, relative heterotopic bone volume was assessed by MicroCT relative to the number of BMP2-producing cells injected (Fig. 6). Results show that there is an increase in bone formation from 10^4 to 10^6 injected cells. Comparable results were achieved when either transduced MC3T3 cells were injected into immune-competent (C57BL/6) mice or when transduced MRC-5 cells were injected into immuno-incompetent (NOD/SCID) mice.

A

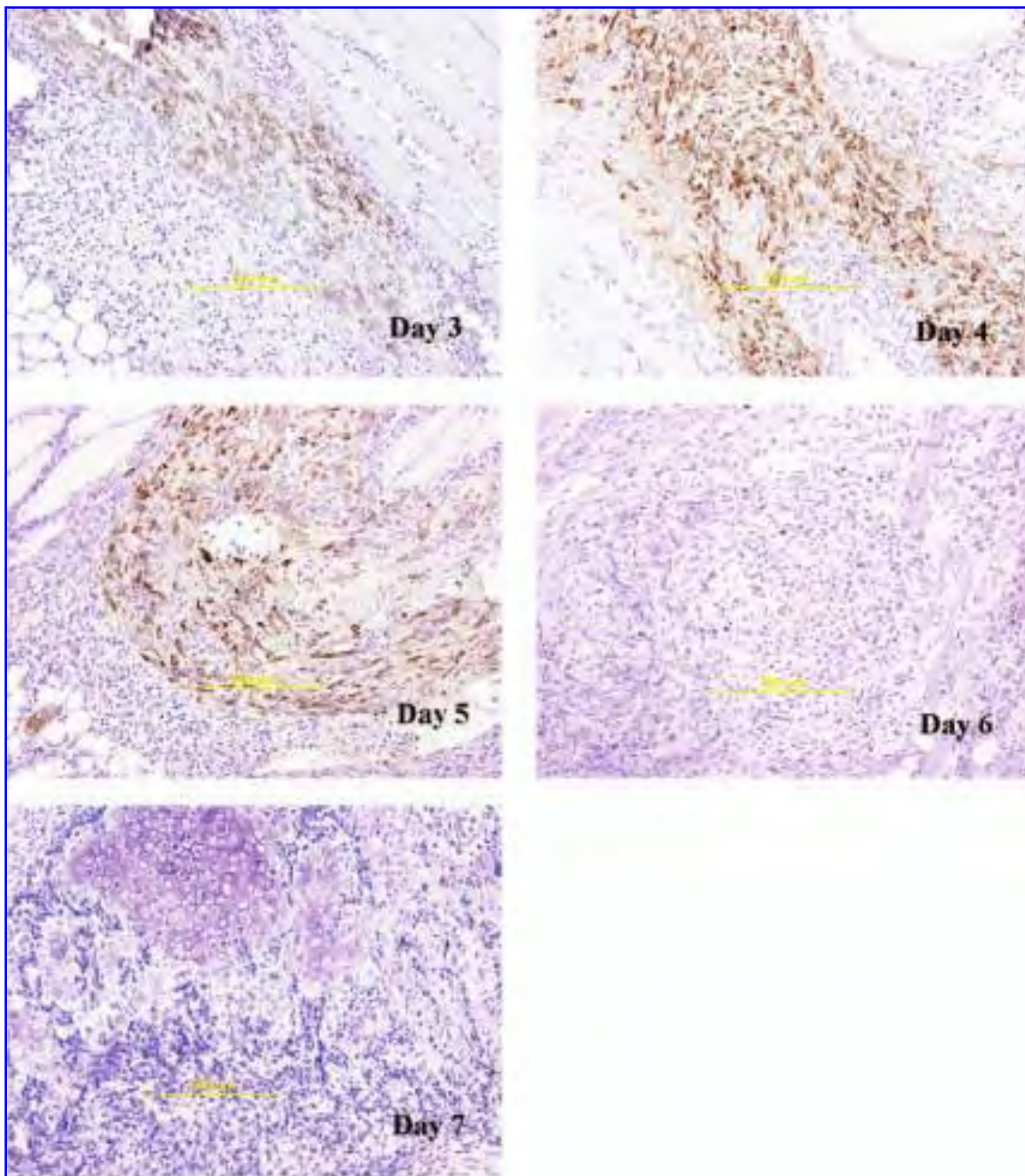


FIG. 2. Immunohistochemistry for human mitochondrial (A) and adenoviral hexon (B) proteins. (A) Staining for human mitochondrial protein on NOD/SCID sections taken from days 3 to 7 demonstrates positivity within the transduced cells from days 3 to 5, whereas the sections from days 6 to 7 are negative, indicating the absence of delivery cells. (B) Low-power photomicrographs of slides stained for hexon, taken from days 3 to 7. Positivity is noted within the transduced cells from days 3 to 5, whereas the day 6 section is weakly positive and the day 7 section is negative, indicating the absence of delivery cells. (Immunohistochemistry; original magnification, $\times 40$.)

DISCUSSION

The study presented here provides a detailed comparison between two different gene therapy models producing rapid bone formation at a directed site. Both systems employ the efficient but transient expression of BMP2 through a cell-based gene

therapy approach, and appear to produce localized bone capable of remodeling into a mature structure. Interestingly, both the immune-compromised (NOD/SCID) and immune-competent (C57BL/6) models yielded identical temporal, morphologic, and volumetric measurements of the bone formation. In all cases transient expression of BMP2 within the tissues led to

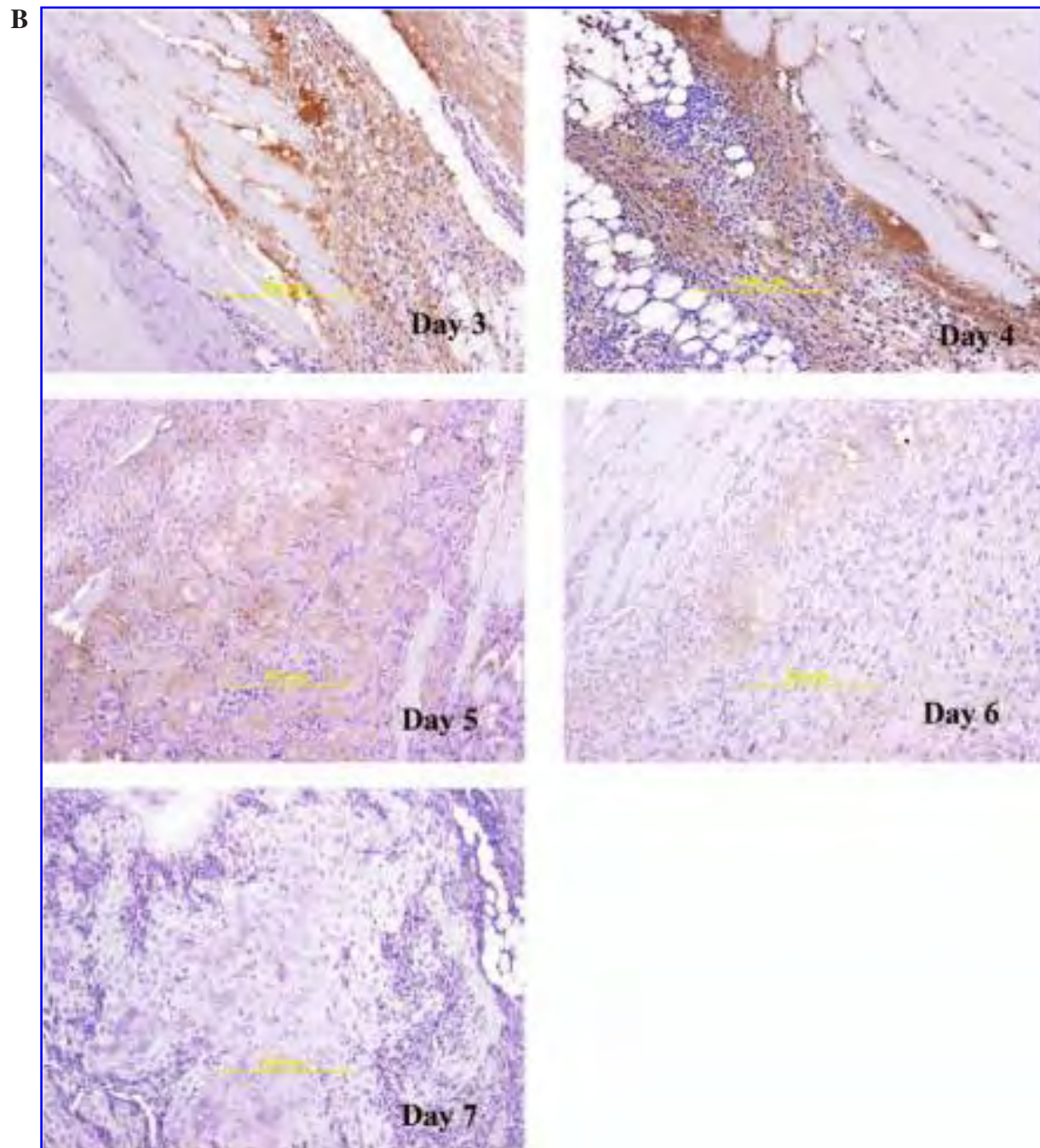


FIG. 2B. *Continued.*

rapid endochondral bone formation in which mineralized bone was detected 7 days after induction.

Previous studies delivering BMP2 by a cell-based gene therapy approach, in which the cells were transduced with first-generation adenoviral vectors, demonstrated bone formation only in immune-compromised animals (Alden *et al.*, 1999). Similar results were observed by Okubo *et al.* (2000) and Sonobe *et al.* (2002), who observed endochondral bone formation only in immunosuppressed rats but not in immune-competent animals. In more recent studies, Sonobe *et al.* (2004), used collagen as a

biomaterial to mask the host immune response and suggested this was a requirement for bone formation in immune-competent animals. In other studies investigators attempted to mask severe inflammatory responses by inclusion of immunosuppressants such as FK506 or cyclosporin A (Okubo *et al.*, 2000; Kaihara *et al.*, 2004).

Here we compare endochondral bone formation in both immune-compromised and immune-competent mice and demonstrate the equivalent nature of these systems. Our data suggest that immunogenicity and clearance of the adenovirus-trans-

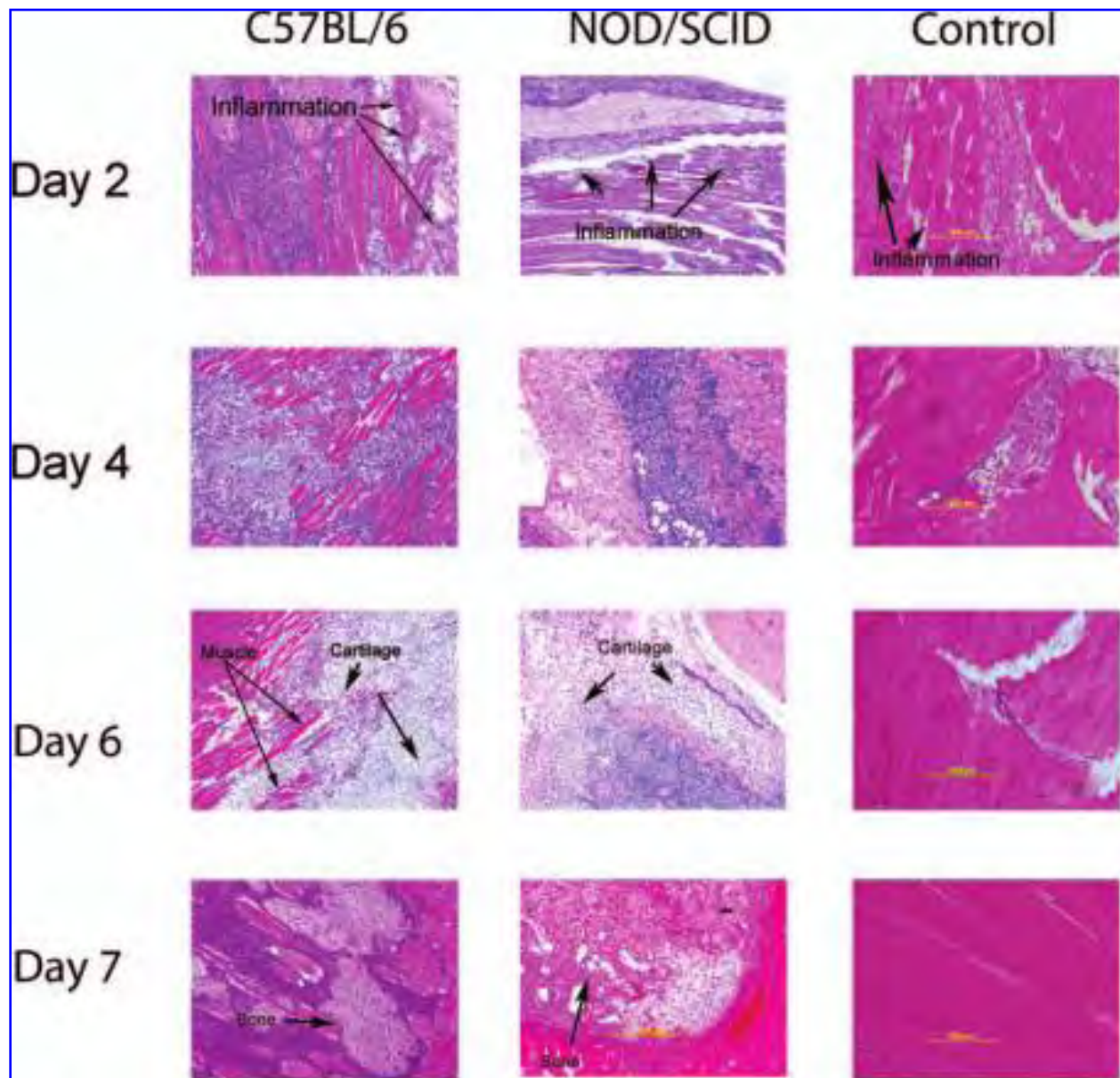


FIG. 3. Photomicrographs from the first week in both experimental (NOD/SCID and C57BL/6) and control animals. Day 2, an inflammatory infiltrate is observed in both experimental and control animals; day 4, the experimental sections for both models no longer match the control sections. The experimental sections show a significant increase in the number of cells within the tissues whereas cell numbers appear greatly reduced in the control section; days 6–7, an orderly maturation of the cartilage component is seen, with progression to bone in both experimental sections, whereas cell numbers in the control section steadily decline. (Hematoxylin and eosin; original magnification, $\times 10.5$.)

duced cells do not interfere with the osteoinductive nature of BMP2. Using set parameters to obtain equivalent functional BMP2 production in the two systems, we injected MRC-5 cells into NOD/SCID animals and MC3T3 cells into C57BL/6 mice. We then compared the temporal formation of bone and morphologic features in the two different models. Bone formation was essentially the same in each of the models.

Thus this cell-based BMP2 gene therapy system has several unique properties that set it apart from other cell and gene therapies. First, long-term expression of the transgene is not a requirement, as evidenced by the significant endochondral bone

formation, even with rapid clearing of BMP2-transduced delivery cells. The ability of BMP2 to induce endochondral bone formation through a trigger-type mechanism has also been demonstrated by others (Koh *et al.*, 2006). This property provides significant advantages over other gene therapy targets, which require long-term persistence of the transgene and have limited ability for readministration. Even the helper-dependent adenovirus with its lessened immunogenicity has not solved the problem (Koehler *et al.*, 2003).

Another issue in these gene therapy systems is the fate of the cells used to introduce BMP2 into the local microenviron-

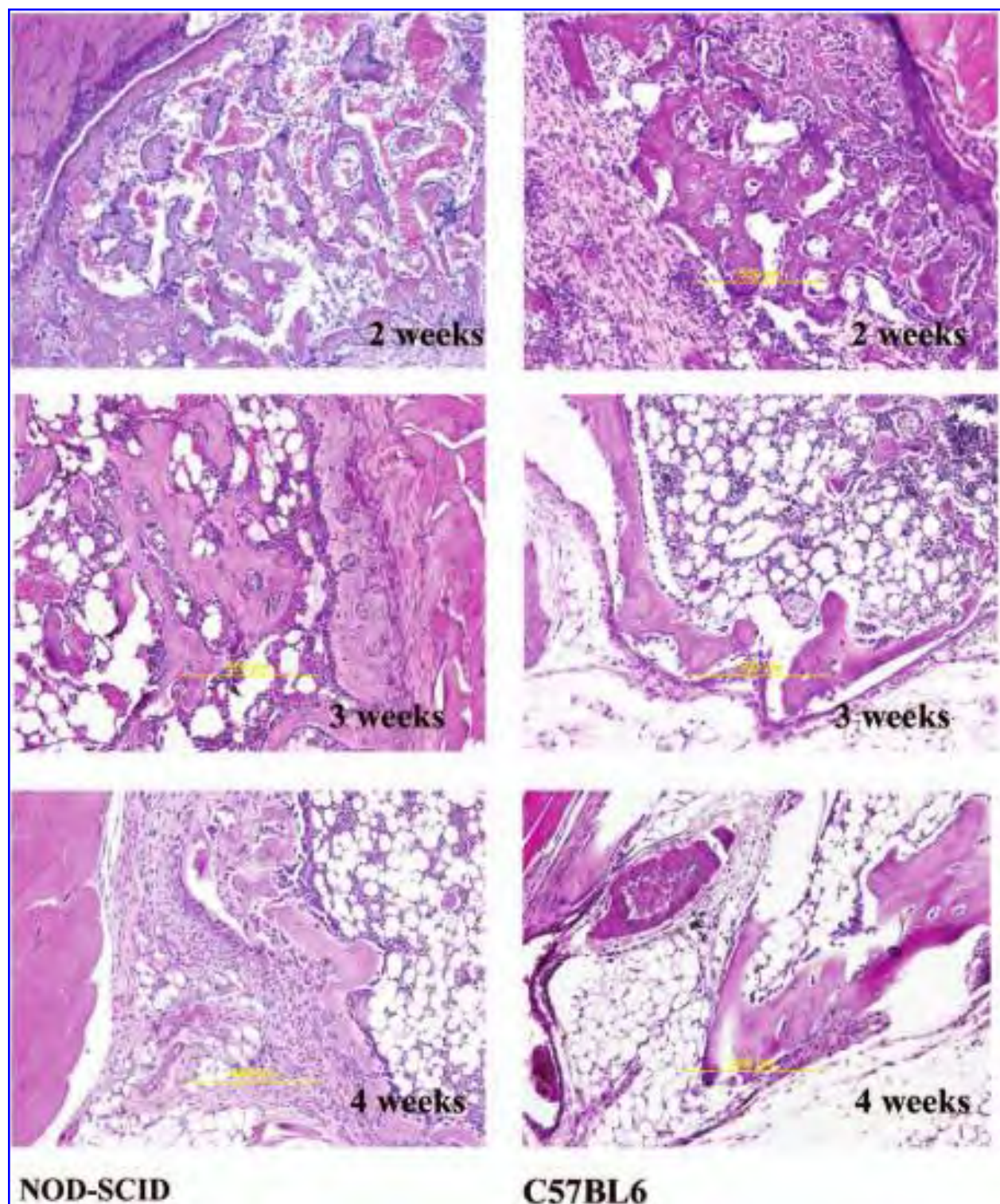
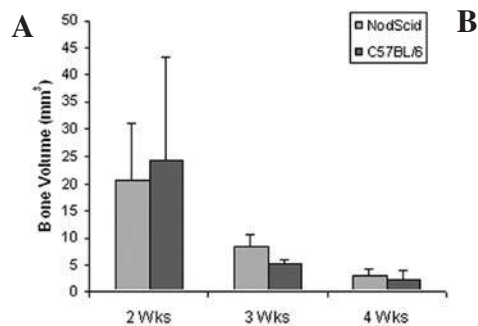


FIG. 4. Long-term analysis of bone formation (2–4 weeks). NOD/SCID sections (*left*) demonstrate well-formed bone with osteoblastic and osteoclastic activity that results in a presumptive marrow cavity by 4 weeks (*bottom left*). C57/BL6 sections (*right*) follow an identical patterning and remodeling that also results in a presumptive marrow cavity. (Hematoxylin and eosin; original magnification, $\times 100$.)

ment. In our cell-based gene therapy systems, the adenovirus-transduced cells serve only to produce BMP2 and are not part of the bone that is created, which is derived entirely from the host. Thus the adenovirus transduction and eventual clearing do

not affect the final bone production. We demonstrate here that the transduced cells completely cleared within 7 days of injection regardless of whether the mouse has a complete immune system. These findings are consistent with studies by Drago



B

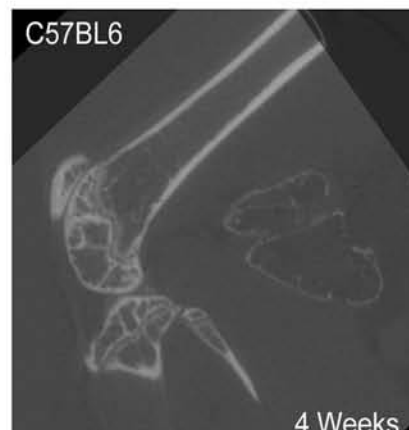
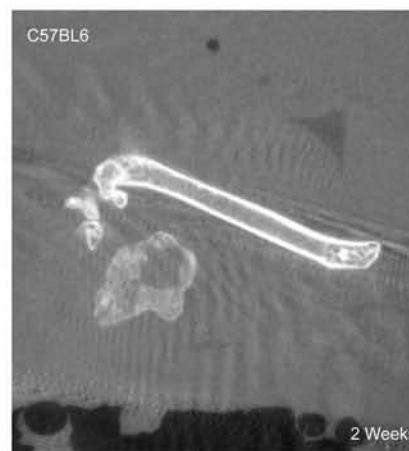
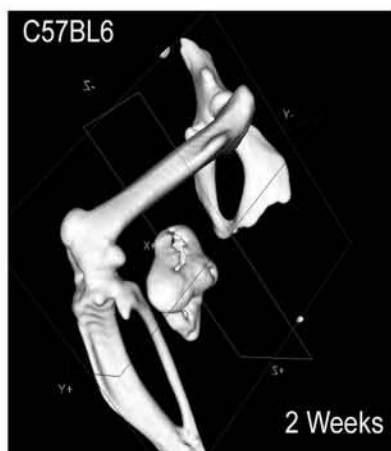
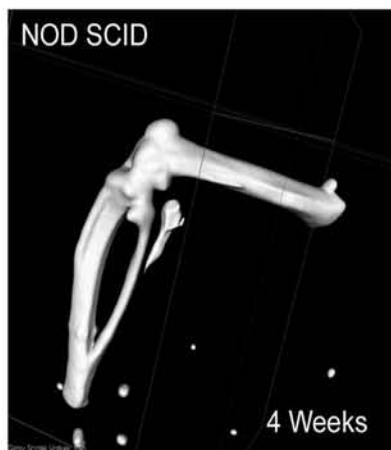
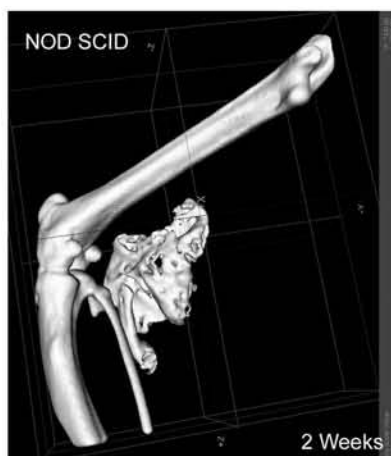
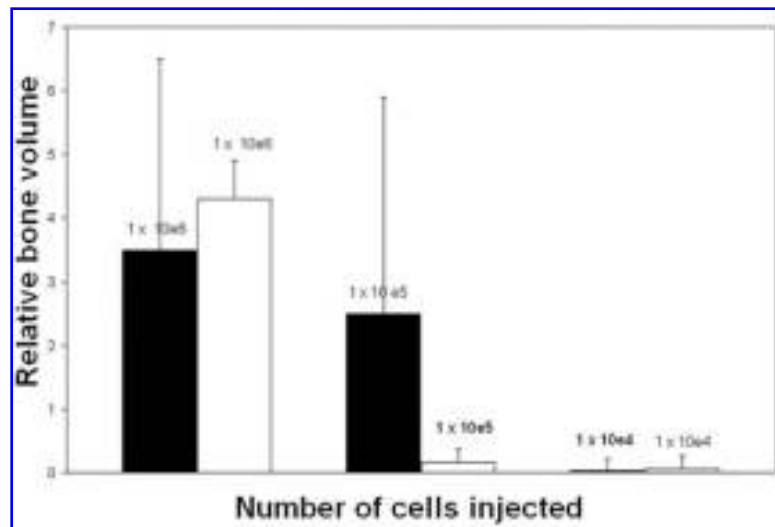


FIG. 5. Graphical representation of heterotopic bone volumes measured by MicroCT. (A) Bone volumes in both systems remain relatively similar and both systems show a significant decrease in overall bone volume from 2 to 4 weeks. (B) Three-dimensional and two-dimensional reconstructions: MicroCT images of bone formed at 2 and 4 weeks postinjection with BMP2 in NOD/SCID and C57BL/6 animals.

FIG. 6. Bone formation as a function of the number of injected BMP2-producing cells. Either 1×10^6 , 1×10^5 , or 1×10^4 BMP2-producing MRC-5 cells were injected into NOD/SCID mice (solid columns) or the same numbers of BMP2-producing MC3T3 cells were injected into C57BL/6 mice (open columns) ($n = 4$). Bone volumes were measured by MicroCT after 2 weeks.



et al. (2005), in which the authors found that inclusion of stem cells isolated from human adipose tissues as delivery cells for the BMP2 did not contribute to the newly forming bone. Similarly, Engstrand *et al.* (2000) have demonstrated that delivery of retrovirally transduced W20-17 cells led to significant bone formation but that the transduced cells themselves were rapidly cleared less than 1 week postimplantation. We have shown in several publications that under our conditions, the injected cells are not incorporated into the heterotopic bone that is formed. We have done this by staining for a human marker when transduced human cells were injected into NOD/SCID mice (Gugala *et al.*, 2003; Olmsted-Davis *et al.*, 2003) and by staining for hexon (Fouletier-Dilling *et al.*, 2005) when adenovirus-transduced mouse cells were injected into normal mice. Immunodetection of hexon protein as a means for detecting clearance of cells from immunocompetent mice is based on several publications showing that first-generation adenoviral vector-transduced cells are rapidly cleared from animals because of vector leakiness and the immune response (Yang and Wilson, 1996; Yang *et al.* 1996a–c). Thus the data suggest that in our hands the transduced cells function only as a means of secreting BMP2 and are not necessary components of the bone structures. However, this does not rule out their potential participation under certain circumstances; it only suggests that their contribution is not essential. Thus, the type of delivery cell can be chosen on the basis of other issues such as ease of acquisition, immunogenicity, and ease of transduction rather than on ability to function as an osteoprogenitor. However, we can envisage some conditions under which the injected cells may be incorporated into the final product. For instance, incomplete transduction of the injected cells may allow untransduced cells to incorporate into bone whereas the transduced cells are destined for immune destruction. This latter phenomenon was first described by Wilson and colleagues (Yang *et al.*, 1994), who noted that “first-generation adenovirus vectors” were in fact leaky. However, osteoprogenitors capable of responding to the local BMP2 may be capable of differentiating into osteoblasts, whereas the transduced cells are actually destroyed. Because our systems are not identical to those who have published incorporation of the cells into bone, it is difficult to determine the exact mechanistic differences, but this certainly could be one explanation.

Alternatively, others developing cell-based gene therapy approaches in different models have found that the cells do contribute to the newly forming bone. Lee *et al.* (2001) demonstrated that muscle-derived cells and bone marrow stromal cells could still contribute to newly forming bone even though they functioned as delivery cells. Moutsatsos *et al.* (2001) used the C3H10T1/2 mesenchymal stem cell line engineered to express high levels of BMP2 protein and showed that these cells were able to contribute to bone healing, beyond recruitment of host-derived cells. Perhaps the lack of viral transduction of these cells aided in their ability to undergo osteogenesis and contribute to bone. Gamradt *et al.* (2006) suggested that mesenchymal stem cells transduced with first-generation adenoviral vectors could also contribute to newly forming bone as functional osteoblasts. Interestingly, in these studies, the authors tagged the BMP2 with a Myc epitope and thus the authors tracked secreted BMP2 rather than the delivery cells themselves. Although the cells were delivered in a collagen sponge that perhaps protected the delivery cells to some extent, the authors could demonstrate the presence of tagged BMP2 protein up to 2 weeks after delivery. It is unclear whether the tag may have stabilized the protein or whether in their system the delivery cells actually undergo osteogenesis.

However, here we present data that demonstrate the ability of BMP2 to rapidly form bone without requiring a specific delivery cell. Thus the choice of delivery cells can be based on factors other than those associated with bone formation. This finding greatly enhances the versatility of the system, in that one can select a cell type based on manufacturing properties as well as versatility in the general population. The ability to develop a single qualified cell type that could be used universally in the general population would greatly reduce the cost and time associated with this therapy, thus allowing for more widespread applications.

ACKNOWLEDGMENTS

This work was funded in part by the U.S. Army (grant DAMD W81XWH-04-1-0068) and by the National Institutes of Health (grant 5RO1 EB005173-02).

AUTHOR DISCLOSURE STATEMENT

No competing financial interests exist.

REFERENCES

- ALDEN, T.D., PITTMAN, D.D., HANKINS, G.R., BERES, E.J., ENGH, J.A., DAS, S., HUDSON, S.B., KERNS, K.M., KALLMES, D.F., and HELM, G.A. (1999). *In vivo* endochondral bone formation using a bone morphogenetic protein 2 adenoviral vector. *Hum. Gene Ther.* **10**, 2245–2253.
- BONADIO, J., SMILEY, E., PATIL, P., and GOLDSTEIN, S. (1999). Localized, direct plasmid gene delivery *in vivo*: Prolonged therapy results in reproducible tissue regeneration. *Nat. Med.* **5**, 753–759.
- BOSCH, P., FOULETIER-DILLING, C., OLMSTED-DAVIS, E.A., DAVIS, A.R., and STICE, S.L. (2006). Efficient adenoviral-mediated gene delivery into porcine mesenchymal stem cells. *Mol. Reprod. Dev.* **73**, 1393–1403.
- CHRIST, M., LUSKY, M., STOECKEL, F., DREYER, D., DIETERLE, A., MICHOU, A.I., PAVIRANI, A., and MEHTALI, M. (1997). Gene therapy with recombinant adenovirus vectors: Evaluation of the host immune response. *Immunol. Lett.* **57**, 19–25.
- DAVIS, A.R., WIVEL, N.A., PALLADINO, J.T., TAO, L., and WILSON, J.M. (2000). Construction of adenoviral vectors. *Methods Mol. Biol.* **135**, 1219–1230.
- DRAGOO, J.L., LIEBERMAN, J.R., LEE, R.S., DEUGARTE, D.A., LEE, Y., ZUK, P.A., HEDRICK, M.H., and BENHAIM, P. (2005). Tissue-engineered bone from BMP2-transduced stem cells derived from human fat. *Plastic Reconstr. Surg.* **115**, 1665–1673.
- ENGSTRAND, T., DALUISKI, A., BAHAMONDE, M.E., MELHUS, H., and LYONS, K.M. (2000). Transient production of bone morphogenetic protein 2 by allogeneic transplanted transduced cells induces bone formation. *Hum. Gene Ther.* **11**, 205–211.
- FOULETIER-DILLING, C.M., BOSCH, P., DAVIS, A.R., SHAFER, J.A., STICE, S.L., GUGALA, Z., GANNON, F.H., and OLMSTED-DAVIS, E.A. (2005). Novel compound enables high-level adenovirus transduction in the absence of an adenovirus specific receptor. *Hum. Gene Ther.* **16**, 1287–1297.
- GAMRADT, S.C., ABE, N., BHAMONDE, M.E., LEE, Y.-P., NELSON, S.D., LYONS, K.M., and LIBERMAN, J.R. (2006). Tracking expression of virally mediated BMP2 in gene therapy for bone repair. *Clin. Orthop. Relat. Res.* **450**, 238–245.
- GAZIT, D., TURGEMAN, G., KELLEY, P., WANG, E., JALENAK, M., ZILBERMAN, Y., and MOUTSATSOS, I. (1999). Engineered pluripotent mesenchymal cells integrate and differentiate in regenerating bone: A novel cell-mediated gene therapy. *J. Gene Med.* **1**, 121–133.
- GUGALA, Z., OLMSTED-DAVIS, E.A., GANNON, F.H., LINDSEY, R.W., and DAVIS, A.R. (2003). Osteoinduction by *ex vivo* adenovirus-mediated BMP2 delivery is independent of cell type. *Gene Ther.* **10**, 1289–1296.
- KAIHARA, S., BESSHO, K., OKUBO, Y., SONOBE, J., KAWAI, M., and IIZUKA, T. (2004). Simple and effective osteoinduction gene therapy by local injection of a bone morphogenetic protein-2 expressing recombinant adenoviral vector and FK506 mixture in rats. *Gene Ther.* **11**, 439–447.
- KOEHLER, D.R., SAJJAN, U., CHOW, Y.H., MARTIN, B., KENT, G., TRANSWELL, A.K., MCKERLIE, C., FORSTNER, J.F., and HU, J. (2003). Protection of Cfr knockout mice from acute lung infection by a helper-dependent adenoviral vector expressing Cfr in airway epithelia. *Proc. Natl. Acad. Sci. U.S.A.* **100**, 15364–15369.
- KOH, J.T., GE, C., ZHAO, M., WANG, Z., KREBSBACH, P.H., ZHAO, Z., and FRANCESCHI, R.T. (2006). Use of a stringent dimerizer-regulated gene expression system for controlled BMP2 delivery. *Mol. Ther.* **14**, 684–691.
- LEE, J.Y., MUSGRAVE, D., PELINKOVIC, D., FUKUSHIMA, K., CUMMINS, J., USAS, A., ROBBINS, P., FU, F.H., and HUARD, J. (2001). Effect of bone morphogenetic protein-2 expressing muscle-derived cells on healing of critical-sized bone defects in mice. *J. Bone Joint Surg.* **83**, 1032–1039.
- LEE, J.Y., PENG, H., USAS, A., MUSGRAVE, D., CUMMINS, J., PELINKOVIC, D., JANKOWSKI, R., ZIRAN, B., ROBBINS, P., and HUARD, J. (2002). Enhancement of bone healing based on *ex vivo* gene therapy using human muscle-derived cells expressing bone morphogenetic protein 2. *Hum. Gene Ther.* **13**, 1201–1211.
- LIEBERMAN, J.R., LE, L.Q., WU, L., FINERMAN, G.A., BERK, A., WITTE, O.N., and STEVENSON, S. (1998). Regional gene therapy with a BMP-2-producing murine stromal cell line induces heterotopic and orthotopic bone formation in rodents. *J. Orthop. Res.* **16**, 330–339.
- MALLAM, J.N., HURWITZ, M.Y., MAHONEY, T., CHEVEZ-BARRIOS, P., and HURWITZ, R.L. (2004). Efficient gene transfer into retinal cells using adenoviral vectors: Dependence on receptor expression. *Invest. Ophthalmol. Vis. Sci.* **45**, 1680–1687.
- MOLINIER-FRENKEL, V., LENGAGNE, R., GADEN, F., HONG, S.S., CHOPPIN, J., GAHERY-SEGARD, H., BOULANGER, P., and GUILLET, J.G. (2002). Adenovirus hexon protein is a potent adjuvant for activation of a cellular immune response. *J. Virol.* **76**, 127–135.
- MOUTSATSOS, I.K., TURGEMAN, G., ZHOU, S., KURKALLI, B.G., PELLE, G., TZUR, L., KELLEY, P., STUMM, N., MI, S., MULLER, R., ZILBERMAN, Y., and GAZIT, D. (2001). Exogenously regulated stem cell-mediated gene therapy for bone regeneration. *Mol. Ther.* **3**, 449–451.
- MUSGRAVE, D.S., BOSCH, P., GHIVIZZANI, P.D., ROBBINS, P.D., EVANS, C.H., and HUARD, J. (1999). Adenovirus-mediated direct gene therapy with bone morphogenetic protein-2 produces bone. *Bone* **24**, 541–547.
- NIYIBIZI, C., WANG, S., MI, Z., and ROBBINS, P.D. (2004). The fate of mesenchymal stem cells transplanted into immunocompetent neonatal mice: implications for skeletal gene therapy via stem cells. *Mol. Ther.* **9**, 955–963.
- OKUBO, Y., BESSHO, K., FUJIMURA, K., IIZUKA, T., and MIYATAKE, S. (2000). Osteoinduction by bone morphogenetic protein-2 via adenoviral vector under transient immunosuppression. *Biochem. Biophys. Res. Commun.* **267**, 382–387.
- OLMSTED, E.A., BLUM, J.S., RILL, D., YOTNDA, P., GUGALA, Z., LINDSEY, R.W., and DAVIS, A.R. (2001). Adenovirus-mediated BMP2 expression in human bone marrow stromal cells. *J. Cell Biochem.* **82**, 11–21.
- OLMSTED-DAVIS, E.A., GUGALA, Z., GANNON, F.H., YOTNDA, P., McALHANY, R.E., LINDSEY, R.W., and DAVIS, A.R. (2002). Use of a chimeric adenovirus vector enhances BMP2 production and bone formation. *Hum. Gene Ther.* **13**, 1337–1347.
- OLMSTED-DAVIS, E.A., GUGALA, Z., CAMARGO, F., GANNON, F.H., JACKSON, K., KIENSTRA, K.A., SHINE, H.D., LINDSEY, R.W., HIRSCHI, K.K., GOODELL, M.A., BRENNER, M.K., and DAVIS, A.R. (2003). Primitive adult hematopoietic stem cells can function as osteoblast precursors. *Proc. Natl. Acad. Sci. U.S.A.* **100**, 15877–15882.
- OLMSTED-DAVIS, E.A., GANNON, F.H., OZEN, M., ITTMANN, M.M., GUGALA, Z., HIPPE, J.A., MORAN, K.M., FOULETIER-DILLING, C.M., SCHUMARA-MARTIN, S., LINDSEY, R.W., HEGGENESS, M.H., BRENNER, M.K., and DAVIS, A.R. (2007). Hypoxic adipocytes pattern early heterotopic bone formation. *Am. J. Pathol.* **170**, 1–13.
- SHAFER, J., DAVIS, A.R., GANNON, F.H., FOULETIER-DILLING, C.M., LAZARD, Z., MORAN, K., GUGALA, Z., OZEN, M.,

- ITTMANN, M., HEGGENESS, M. H., and OLMSTED-DAVIS, E.A. (2007). Oxygen tension directs chondrogenic differentiation of myelo-monocytic progenitors during endochondral bone formation. *Tissue Eng.* **13**, 2011–2019.
- SONOBE, J., BESSHO, K., KAIHARA, S., OKUBO, Y., and IIZUKA, T. (2002). Bone induction by BMP2 expressing adenoviral vector in rats under treatment with FK506. *J. Musculoskel. Res.* **6**, 23–29.
- SONOBE, J., OKUBO, Y., KAIHARA, S., MIYATAKE, S., and BESSHO, K. (2004). Osteoinduction by bone morphogenetic protein 2-expressing adenoviral vector: Application of biomaterial to mask the host immune response. *Hum. Gene Ther.* **15**, 659–668.
- THIES, R.S., BAUDUY, M., ASHTON, B.A., KURTZBERG, L., WOZNEY, J.M., and ROSEN, V. (1992). Recombinant human bone morphogenetic protein-2 induces osteoblastic differentiation in W-20-17 stromal cells. *Endocrinology* **130**, 1318–1324.
- ULUDAG, H., GAO T., PORTER T.J., FRIESS W. and WOZNEY J.M. (2001). Delivery systems for BMPs: Factors contributing to protein retention at an application site. *J. Bone Joint Surg.* **83**, 128–135.
- URIST, M.R. (1965). Bone: Formation by autoinduction. *Science* **150**, 893–899.
- WEISS, K.R., COOPER, G.M., JADLOWIEC, J.A., MCGOUGH, R.L., and HUARD, J. (2006). VEGF and BMP expression in mouse osteosarcoma cells. *Clin. Orthop. Relat. Res.* **450**, 111–117.
- WOZNEY, J.M., ROSEN, V., CELESTE, A.J., MITSOCK, L.M., WHITTERS, M.J., KRIZ, R., HEWICK, R., and WANG, E.A. (1988). Novel regulators of bone formation: Molecular clones and activities. *Science* **242**, 1528–1534.
- YANG, Y., and WILSON, J.M. (1996). CD40 ligand-dependent T cell activation: Requirement of B7-CD28 signaling through CD40. *Science* **273**, 1862–1864.
- YANG, Y., NUNES, F.A., BERENCSI, K., GONCZOL, E., ENGELHARDT, J.F., and WILSON, J.M. (1994). Inactivation of E2a in recombinant adenoviruses improves the prospect for gene therapy in cystic fibrosis. *Nat. Genet.* **7**, 362–369.
- YANG, Y., GREENOUGH, K., and WILSON, J.M. (1996a). Transient immune blockade prevents formation of neutralizing antibody to recombinant adenovirus and allows repeated gene transfer to mouse liver. *Gene Ther.* **3**, 412–420.
- YANG, Y., SU, Q., GREWAL, I.S., SCHILZ, R., FLAVELL, R.A., and WILSON, J.M. (1996b). Transient subversion of CD40 ligand function diminishes immune responses to adenovirus vectors in mouse liver and lung tissues. *J. Virol.* **70**, 6370–6377.
- YANG, Y., SU, Q., and WILSON, J.M. (1996c). Role of viral antigens in destructive cellular immune responses to adenovirus vector-transduced cells in mouse lungs. *J. Virol.* **70**, 7209–7212.

Address reprint requests to:
Dr. Alan R. Davis
Departments of Pediatrics
Baylor College of Medicine
Houston, TX 77030

E-mail: ardavis@bcm.tmc.edu

Received for publication December 14, 2006; accepted after revision June 11, 2007.

Published online: August 8, 2007.